

High-Latitude Ocean and Sea Ice Surface Fluxes: Challenges for Climate Research

Mark A. Bourassa¹, Sarah T. Gille², Cecilia Bitz³, David Carlson⁴, Ivana Cerovecki², Carol Anne Clayson^{1,5}, Meghan F. Cronin⁶, Will M. Drennan⁷, Chris W. Fairall⁸, Ross N. Hoffman⁹, Gudrun Magnusdottir¹⁰, Rachel T. Pinker¹¹, Ian A. Renfrew¹², Mark Serreze¹³, Kevin Speer¹, Lynne D. Talley², Gary A. Wick⁸

¹Florida State University, Tallahassee, Florida, USA

²University of California San Diego, La Jolla, California, USA

³University of Washington, Seattle, Washington, USA

⁴British Antarctic Survey, Cambridge, United Kingdom

⁵now at Woods Hole Oceanographic Institution, Woods Hole, Massachusetts, USA

⁶National Oceanic and Atmospheric Administration (NOAA) Pacific Marine Environmental Laboratory, Seattle, Washington, USA

⁷University of Miami, Miami, Florida, USA

⁸NOAA Earth System Research Laboratory, Boulder, Colorado, USA

⁹Atmospheric and Environmental Research, Lexington, Massachusetts, USA

¹⁰University of California Irvine, Irvine, California, USA

¹¹University of Maryland, College Park, Maryland, USA

¹²University of East Anglia, Norwich, United Kingdom

¹³University of Colorado, Boulder, Colorado, USA

Corresponding Author: Sarah Gille, Scripps Institution of Oceanography, University of California San Diego, 9500 Gilman Dr. Mail Code 0230, La Jolla, CA 92093-0230, United States. E-mail: sgille@ucsd.edu

26

27 Short summary: High latitudes present extreme conditions for the measurement and estimation of air–
28 sea fluxes, limiting understanding of related physical processes and feedbacks that are important
29 elements of the Earth’s climate.

30

31 Abstract: Polar regions have great sensitivity to climate forcing; however, understanding of the
32 physical processes coupling the atmosphere and ocean in these regions is relatively poor. Improving
33 our knowledge of high-latitude surface fluxes will require close collaboration among meteorologists,
34 oceanographers, ice physicists, and climatologists and between observationalists and modelers, as well
35 as new combinations of in situ measurements and satellite remote sensing. This article describes the
36 deficiencies in our current state of knowledge about air–sea surface fluxes in high latitudes, the
37 sensitivity of various high-latitude processes to changes in surface fluxes and the scientific
38 requirements for surface fluxes at high latitudes. We inventory the reasons, both logistical and physical,
39 why existing flux products do not meet these requirements. Capturing an annual cycle in fluxes
40 requires that instruments function through long periods of cold polar darkness, often far from support
41 services, in situations subject to icing and extreme wave conditions. Furthermore, frequent cloud cover
42 in high latitudes restricts the availability of surface and atmospheric data from visible and infrared (IR)
43 wavelength satellite sensors. Recommendations for improving high-latitude fluxes include (1)
44 acquiring more in situ observations; (2) developing improved satellite flux observing capabilities; (3)
45 making observations and flux products more accessible; and (4) encouraging flux intercomparisons.

46

47 **1. Introduction**

48 High-latitude climate change can manifest itself in astonishing ways. Arctic sea ice extent at the
49 end of the melt season in September is declining at a mean rate of 12% per decade, with a record

50 seasonal minimum in 2007 (Comiso et al. 2008). In 2001–02, the Larsen B Ice Shelf on the Antarctic
51 Peninsula collapsed in a matter of months (Rignot et al. 2004), and in 2008, the Wilkins Ice Shelf
52 collapsed equally quickly (Scambos et al. 2009). Ocean heat content is rising rapidly in high-latitude
53 regions of both hemispheres (e.g., Gille 2002; Karcher et al. 2003; Purkey and Johnson 2010). In a
54 broad sense, these observed changes are consistent with projections of anthropogenic climate change
55 reported in the Intergovernmental Panel on Climate Change (IPCC) 4th Assessment Report (AR4)
56 (Randall et al. 2007). A common element in high-latitude climate changes is a dependence on surface
57 fluxes, i.e., the exchange of heat, momentum, and material between the ocean, atmosphere, and sea ice.

58 Surface fluxes at high latitudes reflect a broad range of processes, as depicted schematically in Fig.
59 1 (the basic concepts defining surface fluxes are outlined in Sidebar #1.) Were the magnitude and
60 variations in these fluxes well known, they would provide enormous insights into aspects of the climate
61 system, including the evolution of sea ice mass, meridional heat and salinity transport, and large-scale
62 variability within the climate system (e.g. the North Atlantic Oscillation, the Annular Modes, the
63 Pacific Decadal Oscillation, and even ENSO teleconnections). However, the magnitude and variations
64 of surface fluxes at high latitudes are poorly known, leading to large uncertainties in the present
65 climate state at high latitudes (e.g., Dong et al. 2007; Cerovecki et al. 2011b; Vancoppenolle et al. 2011;
66 Kwok and Untersteiner 2011) and limiting our ability to validate climate models used to project
67 twenty-first-century climate (Christensen et al. 2007). Improving our knowledge of high-latitude
68 surface fluxes will require close collaboration among meteorologists, oceanographers, ice physicists,
69 and climatologists; new combinations of in situ measurements and satellite remote sensing (e.g.,
70 improvements upon Bourassa et al. 2010b); and close interaction between observationalists and
71 modelers.

72 This article, an outcome of the US CLIVAR Working Group on High Latitude Surface Fluxes
73 Workshop (<http://www.usclivar.org/hlat.php>), describes the scientific requirements for surface fluxes at
74 high latitudes, which we define to include the Arctic and the Subarctic Ocean, and the Southern Ocean.

75 We inventory the reasons, both logistical and physical, why existing flux products do not meet these
76 requirements. We conclude with suggestions for improving high-latitude flux estimates. Our focus is
77 on ocean–atmosphere fluxes and radiative fluxes over high-latitude seas and sea ice. We do not
78 consider fluxes over land surfaces or freshwater fluxes from land to ocean. The recent SWIPA (Snow,
79 Water, Ice, Permafrost of the Arctic) assessment (Arctic Monitoring and Assessment Programme, 2011,
80 <http://www.amap.no/swipa/>) provides an up-to-date description of surface and lateral fluxes and net
81 mass changes of the Greenland ice sheet, and addresses requirements for measuring carbon fluxes over
82 tundra and terrestrial permafrost regions.

83

84 **2. Unique Challenges and Desired Accuracies**

85 High-latitude fluxes differ markedly from those in temperate regions because of the presence of ice,
86 frequent high wind speeds (Fig. 2), low winter temperatures, both large and small seasonal temperature
87 ranges, and pronounced variability on local scales, particularly along sea ice margins and leads (linear
88 openings in the ice cover). As a result, physical understanding gained in temperate regions is not
89 necessarily applicable to high latitudes. The high-latitude environment also poses logistical challenges.
90 Capturing an annual cycle in fluxes, for example, requires that instruments function through long
91 periods of cold polar darkness, often far from support services, in situations subject to icing and
92 extreme wave conditions. These logistical challenges are reflected in a relative paucity of standard
93 surface and upper-air meteorological data and an almost complete absence of moored¹ or free-drifting
94 sensor systems in large areas of the polar oceans, particularly those covered with seasonal or perennial
95 ice. Frequent cloud cover in high latitudes restricts the availability of surface and atmospheric data
96 from visible and infrared (IR) wavelength satellite sensors. This lack of information reduces the quality

1 The first meteorological mooring in the Southern Ocean was deployed in March 2010, at 140°E, 47° S, by the Australian Integrated Marine Observing System (Trull et al. 2010). It measures wind, temperature, humidity, atmospheric pressure, solar radiation, and precipitation but not turbulent fluxes. A second mooring that was deployed in the Agulhas Return Current at 30°E, 38.5°S in November 2010, broke loose from its anchor after less than 7 weeks. Similar difficulties occurred in the northern high latitudes (Moore et al. 2008),

97 of data assimilation products from numerical weather prediction (NWP) centers such as the European
98 Centre for Medium-Range Weather Forecasts (ECMWF) and the National Centers for Environmental
99 Prediction (NCEP). More numerous and more accurate in situ and satellite observations are required.

100 In view of the importance of high-latitude surface fluxes and the challenges in measuring them, it is
101 reasonable to ask what accuracy is needed for different applications. Sidebar #2 highlights a wide
102 range of applications that make use of surface flux observations. In Fig. 3, we summarize flux
103 accuracy requirements that have emerged from discussions with researchers representing atmospheric
104 science, oceanography, and Arctic sea ice physics. The consensus is that the shortcomings in high-
105 latitude observing systems and NWP are too great to allow for the determination of precise accuracy
106 requirements for most processes. The values shown in Fig. 3 are therefore rough estimates to be
107 refined as observing systems and NWP systems improve.

108 Climate processes occur on a suite of space and time scales with different accuracy requirements
109 and challenges (Fig. 3). For measurements of smaller scale processes ($<100\text{km}$), such as those
110 governing a cold-air outbreak off the coast of Greenland (see Fig. 4; Petersen and Renfrew 2009), in
111 situ observations of variables such as temperature and wind speed are typically well sampled, and
112 observational error is dominated by random errors. However, NWP products can have large errors on
113 these small scales because they cannot resolve small-scale features (Fig. 4). For large-scale processes,
114 such as zonally averaged monthly fluxes (Fig. 5), individual observations are averaged, which reduces
115 random errors by a factor of the square root of the number of independent observations, meaning that
116 random errors have little impact. Instead errors are dominated by biases in observations (which are
117 typically small compared to random uncertainty in individual observations) or biases in
118 parameterizations. On the large scale, fluxes from NWP are typically limited by biases in
119 parameterizations and related physical assumptions. Therefore, for the smaller scale processes it is
120 essential to have accurate individual observations or model representation, whereas larger scale studies
121 require low biases. Importantly, some processes do not respond linearly to the forcing; for such

122 processes it is critically important to properly represent the distribution of fluxes. In current products
123 these distributions differ enormously as demonstrated by the discrepancies in the median as well as the
124 5th and 95th percentiles of sensible and latent heat flux estimates shown in Fig. 5.

125

126 **3. Improving the Accuracy of Fluxes**

127 The specific shortcomings in high-latitude surface fluxes result from a number of distinct issues. Here
128 we discuss problems stemming from flux parameterizations, observational errors, and sampling errors.

129 *a. Flux Parameterizations*

130 Some flux estimates fail in part because they are calculated using parameterizations that have not been
131 optimized for high-latitude conditions. Whereas surface turbulent fluxes can be measured directly with
132 specialized sensors placed on suitable platforms over the ocean (e.g., Ho et al. 2007; Wanninkhof et al.
133 2009), most applications require estimates distributed over a broader range in space and time than can
134 be achieved with dedicated flux sensors. Thus, direct in situ flux observations are used to develop and
135 tune indirect parameterizations, known as *bulk flux algorithms*, which allow fluxes to be calculated
136 from more easily measured variables such as wind speed and sea surface temperature. Bulk flux
137 algorithms have been in use for decades (see e.g., Blanc 1985; Curry et al. 2004). Advances in
138 understanding the physical processes involved in air–sea exchange and in observing technologies have
139 promoted steady improvements in the sophistication and accuracy of these algorithms. Bulk-flux
140 algorithms are also used in retrievals of turbulent fluxes from satellite observations (Bourassa et al.
141 2010b). They have been used extensively to estimate the heat balance of the oceans from historic
142 weather observations from volunteer observing ships (WCRP 2000), and they form the basis for
143 describing the atmosphere–ocean boundary interactions in virtually all climate and NWP models.

144 There are two dominant sources of error in bulk algorithms: 1) the choice of the transfer
145 coefficient and 2) the accuracy of the routinely observed variables used to compute the fluxes. Transfer

146 coefficients for momentum (Fig. 6a), sensible or latent heat flux (Fig. 6b), and gas exchange (Fig. 6c)
147 vary with wind speed, and coefficient estimates derived from different sources can differ dramatically,
148 as the solid lines in Fig. 6 illustrate. The transfer coefficients are largely functions of wind speed
149 (relative to the water surface) and air–sea temperature differences; C_D is also a function of sea state. A
150 problem in high latitudes is the relatively high likelihood of extreme conditions, for which bulk
151 algorithms are less reliably tuned. Regional biases in fluxes occur when some of these dependencies are
152 approximated or ignored (e.g., Renfrew et al. 2002). In some cases, bulk parameterizations may simply
153 be introducing an unnecessary layer of complication in the effort to determine surface fluxes. Accurate
154 retrievals of stress or \mathbf{u}_* (see Table 1) would remove the problems associated with the C_D dependence
155 on sea state (e.g., Fairall et al. 1996; Bourassa 2006). For example, since centimeter-scale radar
156 backscatter is more closely tied to stress than to wind (Bourassa et al. 2010a), scatterometers can
157 probably be tuned to measure stress and hence determine \mathbf{u}_* . Tuning stress retrievals and transfer
158 coefficients for highly atypical conditions, or conditions that are adverse to in situ sensors, will be a
159 challenge given the paucity of observations and the importance of physical processes that are not yet
160 well modeled in current parameterizations: for example, sea spray at very high wind speeds (Andreas et
161 al. 2008), rain (Weissman and Bourassa, 2011), and mixed ice and water (Alam and Curry, 1997).
162 These conditions occur regularly in high latitudes, and are linked to processes that are important to
163 climate.

164 Different challenges arise for estimating radiative fluxes, which include shortwave radiation
165 from the sun and longwave radiation emitted from the ocean surface and from the atmosphere.
166 Shortwave (solar) fluxes are commonly estimated from satellite observations using empirical,
167 statistical, and/or physically based methods (Schmetz 1989, 1991, 1993; Pinker et al. 1995; Whitlock et
168 al. 1995; Wielicki et al. 1995). The downward shortwave flux at the surface depends on the shortwave
169 flux at the top of the atmosphere and on the fraction of this flux that is transmitted through the

170 atmosphere. The transmittance depends on the composition of the atmosphere (e.g., amount of water
171 vapor and ozone, optical thickness of cloud and aerosols), and on the distance the radiation travels
172 through the atmosphere (modified by the solar zenith angle and scattering). The upward shortwave
173 flux at the surface is then calculated by multiplying the surface downward flux by the surface albedo.
174 Uncertainties in the shortwave fluxes stem from the substantial uncertainties in the atmospheric
175 transmittance and surface albedo. Estimates of radiative fluxes from different satellite-based products
176 disagree strongly in polar regions (Fig. 7). Estimates from the Surface Heat Budget of the Arctic
177 Ocean (SHEBA) project and from high-latitude buoy and land stations suggest that satellite-based
178 analysis provide downward shortwave radiative fluxes to within $\sim 10\text{-}40\text{ W m}^{-2}$ of direct surface
179 observations (e.g. Perovich et al. 1999; Curry et al. 2002; Niu et al. 2010; Niu and Pinker 2011). This
180 uncertainty is too large for most climate applications; however, much of this difference could be due to
181 representativeness differences (i.e. due to comparing surface observations at one location in a very
182 inhomogeneous environment to satellite estimates averaged over larger spatial scales.)

183 Estimating longwave surface radiative fluxes from satellites is also challenging. Downwelling long-
184 wave surface radiation is controlled by the vertical profiles of temperature, gaseous absorbers, clouds,
185 and aerosols. In contrast to the tropics, at high latitudes the moisture content of the atmosphere is low.
186 As a result, the high-latitude atmosphere is semitransparent in some infrared bands that are normally
187 opaque (Turner and Mlawer 2010). An especially formidable issue is that the longwave flux depends
188 strongly on the cloud-base height, which is not as yet detectable from satellite, and quantities measured
189 by satellite are not directly correlated to downwelling radiation. Consequently, downwelling longwave
190 radiation is often estimated as a function of a bulk atmospheric temperature approximated by air
191 temperature at the ground and an estimated broadband atmospheric emissivity. For cloudless skies,
192 more than half the longwave flux received at the ground comes from emissions in the lowest 100 m
193 (Zhao et al. 1994), because the lowest atmospheric layers are relatively warmer than higher layers and

194 intercept some of the radiation emitted by higher layers. Estimating the upward longwave flux is more
195 direct and simply calculated from surface temperature and emissivity of the surface.

196 Estimated downward longwave fluxes have been evaluated against surface observations in a
197 number of land-based studies (e.g., König-Langlo and Augstein 1994; Key et al. 1996; Guest 1998;
198 Makshtas et al. 1999) and are typically accurate to $\sim 10\text{-}30 \text{ W m}^{-2}$ at high latitudes (Perovich et al. 1999;
199 Nussbaumer and Pinker, 2011). For example, the parameterization of König-Langlo and Augstein
200 (1994) reproduced the observations with root-mean-square (RMS) differences of less than 16 W m^{-2} .
201 Though these accuracies are reasonable, like the shortwave flux accuracies, they are insufficient to
202 meet the requirements indicated in Fig. 3 for many applications. For short time and small spatial
203 scales, the largest sources of uncertainty in radiative fluxes are thought to stem from algorithm
204 implementation problems associated with issues such as diurnal corrections and radiance-to-flux
205 conversions (Wielicki et al. 1995).

206 Radiative fluxes are also computed as an output from NWP reanalyses (sometimes in
207 combination with satellite data) or global climate models. Model-based approaches have the apparent
208 advantage of providing dynamically consistent fields with all relevant variables including cloud cover
209 and atmospheric aerosol concentrations. However, satellite-based approaches have generally proven
210 more successful than models that resolve scales larger than 100 km. For example, Liu et al. (2005)
211 found that the surface downward shortwave radiative fluxes derived from satellites are more accurate
212 than those from the NCEP and ECMWF reanalysis datasets because of better information on cloud
213 properties. Sorteberg et al. (2007) found that the 20 coupled models used in the IPCC Fourth
214 Assessment Report have large biases in surface fluxes, particularly over marginal ice zones. The
215 models significantly underestimate both downward and upward longwave radiation in winter.

216 Different issues exist for precipitation fluxes. Satellite retrievals are of poor quality over cloudy
217 and snow- and ice-covered surfaces (e.g. Gruber and Levizzani, 2008; Sapiano, 2009), and it appears
218 that better estimates can be obtained from atmospheric reanalyses (Serreze et al. 2005) or from

219 combinations of satellite plus reanalysis and/or station data (Huffman et al. 1997; Xie and Arkin 1997).
220 However, precipitation biases in reanalysis fields can be very large (Serreze and Hurst 2000), in part
221 because of errors in radiative transfer parameterizations, and in part because of model microphysics
222 and transport errors leading to incorrect input to the radiative transfer model.

223

224 ***b. Observation Errors***

225

226 Even if flux parameterizations were perfect, one is still left with the problem of obtaining high-
227 quality observations. Observation error refers to error characteristics of single observations. For some
228 sensors these are serious concerns. For example, gauge errors in measured precipitation for Arctic
229 stations can exceed 100% in winter (Yang, 1999). For other sensors, such as those that are well
230 maintained on ships and buoys, the observations needed for input to bulk formulas have sufficiently
231 small random errors for many applications. Substantial biases can occur due to the lack of important
232 metadata for observations collected on ships, such as the physical height of sensors, and whether the
233 anemometer at the time of observation is on the leeward or windward side of the ship Bradley and
234 Fairall, 2006). Polar conditions are also very harsh on instruments, which can necessitate special
235 equipment or frequent maintenance.

236 Satellite observations vary in reliability. Scatterometer wind observations have consistent
237 accuracies for individual sensors but are not yet intercalibrated, particularly for high wind speeds
238 (Bourassa et al. 2010c). Unfortunately, available scatterometers do not fully resolve the tight gradients
239 that occur along fronts and within strong extratropical cyclones, nor do they provide temporal
240 resolution needed to track rapidly evolving storms. Moreover, since the demise of QuikSCAT in
241 November 2009, researchers have relied more on ASCAT, which is less affected by precipitation but
242 has a narrower swath than QuikSCAT, limiting the view of large-scale storms. In addition, ASCAT is

243 currently calibrated differently than QuikSCAT for 10-meter winds, $U_{10} > 15\text{ms}^{-1}$. For extreme winds
244 found in strong mid-latitude cyclones these difference can exceed 10 m s^{-1} (Bourassa et al. 2010c).

245 Satellites can be quite effective for observing sea surface temperatures (SSTs). Microwave
246 sensors perform well through cloudy conditions, but infrared sensors, which are required to resolve
247 small-scale features, are thwarted by clouds, resulting in little or no high-resolution data in perennially
248 cloudy regions, such as parts of the Southern Ocean. Furthermore, microwave satellite instruments are
249 ineffective closer to a shoreline or ice (areas of great interest) than their resolution. The new generation
250 of SST products optimally blending in situ, microwave, and infrared observations provide a way
251 forward (e.g., Donlon et al. 2007). New satellite observations are improving estimates of surface
252 albedo and aerosols (e.g., Schaaf et al. 2002; Remer et al. 2005; Kahn et al. 2005), although the
253 dominant error source still stems from calibration uncertainties in satellite instruments. There are very
254 large differences between estimates from NWP, satellites, and in situ products (Smith et al. 2010).
255 Recent techniques for retrieving air temperature and humidity (Jackson et al. 2006, 2009; Jackson and
256 Wick 2010; Roberts et al. 2010; Dong et al. 2010) have yielded improved estimates over a wider range
257 of conditions. These retrievals have noise that is mildly worse than in situ observations; however, they
258 have substantial biases over the very cold water that characterizes high latitudes. The impact of these
259 improvements on turbulent fluxes remains to be determined (Bourassa et al. 2010b).

260 Some studies make use of NWP estimates of SST, air temperature, humidity, and other variables
261 to obtain surface fluxes. These estimates typically have large regional biases (Smith et al. 2010).
262 When the NWP parameterizations are implemented in coupled climate models, biases in the input to
263 bulk flux parameterizations can introduce larger errors in the fluxes and feedbacks in the coupled
264 systems. Transfer coefficients in climate models have been modified to account for these biases.
265 However, this type of tuning means that any modeled response to changes in wind, temperature, and
266 humidity is likely inaccurate, which is a serious problem in high latitudes, where several key climate

267 processes (including ocean uptake of heat and water mass transformation) are sensitive to the
268 magnitude of energy fluxes and to the directional stress.

269 Ultimately, improved observations of air–sea temperature differences and measurements of
270 stress will improve the accuracy of CO₂ flux retrievals from satellites. The largest sources of error in
271 CO₂ fluxes are insufficient sampling of the highly variable winds in polar latitudes, large changes in
272 pCO₂ across the air-sea interface in areas of differing biological activity (Martz et al. 2009), and
273 indirect methods of regionally estimating oceanic pCO₂ from satellite observations. These atmospheric
274 and aqueous pCO₂ estimates require ongoing validation from sparse observations collected by research
275 vessels. Satellites currently lack the ability to measure atmospheric pCO₂ with sufficient accuracy at
276 the desired resolution; however, lidar (Wilson et al. 2007) and the Atmospheric Infrared Sounder
277 (AIRS, Engelen et al., 2004; Engelen and McNally, 2005; Engelen and Stephens, 2004; Strow and
278 Hannon, 2009) show promise for the future.

279 For radiative fluxes, observational errors are similarly important. Shi and Long (2004)
280 discussed accuracy limits of ground observations. Clouds are major modulators of the shortwave
281 radiation budgets; however, information on their physical properties and vertical structure is not readily
282 available, particularly in polar regions, in part since ice or snow and low clouds are difficult to
283 distinguish in satellite data. Since, satellites are critical for obtaining estimates of radiative fluxes,
284 particularly for long time scales and large space scales, one important step forward is to compare
285 satellite-based downward surface flux estimates against ground measurements. At most latitude ranges,
286 globally distributed ground measurements have improved over the last 12 years with the advent of the
287 GEWEX Baseline Surface Radiation Network (Ohmura et al. 1998; Michalsky et al. 1999), with recent
288 studies reporting agreement within 10 Wm⁻² on a monthly time scale (e.g., Charlock and Alberta, 1996;
289 Stackhouse et al. 2004). A similar high-latitude network is needed.

290

291

292 *c. Sampling Errors*

293 The third major challenge for obtaining quality surface fluxes is sampling errors. This refers to
294 error characteristics associated with under-sampling natural variability. Important cases of under-
295 sampling also occur when observations are made conditionally, e.g., only in clear or non-precipitating
296 conditions. Under-sampling can result in large and non-Gaussian errors (Gulev et al. 2007a, b) and
297 spatial/temporal inhomogeneity in error characteristics (Schlax et al. 2001). Furthermore, scales smaller
298 than the scale of the observation network will alias onto the larger scales that are resolved. High-
299 latitude sampling errors are large because there are so few observations, and there are large changes in
300 variables over relatively small times and distances. In situ radiative flux data for high latitudes come
301 from land-based radiometer measurements, and there relatively few in situ observations of shortwave
302 or longwave radiative fluxes over high-latitude oceans. Flux moorings have not been deployed
303 routinely in any high-latitude region. In situ ocean data that are available have hence been limited
304 largely to collections from ships. In regions with major shipping routes, volunteer observing ships
305 (VOS) now provide enough data to calculate surface energy fluxes, although monthly averages still
306 have large errors (Berry and Kent, 2011). However, south of 30°S and poleward of 50°N there are few
307 ship observations, coupled with large natural variability, which results in very poor matches between
308 VOS products and satellite products (e.g., Risien and Chelton 2008). For studies of the upper-ocean
309 heat content, profiling Argo floats have been a boon. However, Argo's target of sampling at 10-day
310 temporal resolution and 3° spatial resolution precludes resolving details of spatial and temporal surface
311 flux variations. High-inclination polar orbiting satellites have relatively good sampling in polar
312 regions; however, the natural variability of winds and clouds is also quite large, resulting in large
313 sampling errors. Further, since cloud amount and type is tied to synoptic weather patterns, IR sensors
314 provide only a conditional sampling of meteorological conditions.

315 In some cases relevant data, particularly those affecting radiative fluxes, are simply not part of the
316 observational data stream. The high albedo of snow and ice, together with the cold and fairly dry
317 atmosphere, results in a surface net radiation deficit for most months. Cloud cover typically reduces
318 the radiation deficit (Pietroni et al. 2008) by absorbing upward longwave radiation and reemitting some
319 of it back toward the surface. Thus, Pietroni et al. (2008) concluded that differences in longwave
320 radiation distributions between two Antarctic sites, one near the coast and one in the interior, were
321 strongly related to differences in cloud cover. Cloud-related scattering of shortwave radiation is also
322 unusually important in this region. However, the characteristics of clouds and aerosols in polar
323 regions, and in particular their small-scale variation depending on surface type, are poorly known and
324 not routinely measured (Lubin and Vogelmann 2006).

325 Sampling problems are compounded by the fact that fluxes at high latitudes vary over shorter
326 spatiotemporal scales than fluxes at lower latitudes. For surface turbulent fluxes, length-scales over the
327 high-latitude open ocean are determined by the first baroclinic Rossby radius, which can be 20 km or
328 less (Chelton et al., 1998) and time scales can range from a couple of days to < 6 hours (e.g. Condrón et
329 al., 2008; Jiang et al., 2011), because high-latitude storms evolve quickly. Physics at meter to
330 kilometer scales also matters: breaking waves and whitecaps are of first order importance in production
331 of sea spray (Andreas and Monahan, 2000; Andreas and Emmanuel, 2001; Lewis and Schwartz, 2004;
332 Fairall et al., 2009), in gas transfer (e.g., Woolf, 2005), and of some importance in wind-stress
333 relationships (e.g, Mueller and Veron, 2009).

334 Precipitation is notoriously difficult to determine. For example, Serreze et al. (2005) estimate that
335 at a coarse grid cell resolution of 175 km, obtaining an accurate assessment of the monthly grid cell
336 precipitation requires typically 3–5 stations within the cell, and more in topographically complex areas.
337 However, for the Arctic terrestrial drainage, only 38% of the 175-km grid cells contain even a single
338 station. The situation is much worse over Antarctica, the Southern Ocean, and the Arctic Ocean.
339 Sampling from satellites can have large errors in these regions because time intervals between

340 observations are in many cases too large compared to the variability associated with storm systems.
341 TRMM, the dedicated precipitation mission, does not reach high latitudes, and other satellite products
342 show anomalously high variability poleward of 50° latitude and in ice-covered areas (Sapiano, 2009).
343 Furthermore, satellite observations with large footprints have insufficient spatial resolution to capture
344 the spatial variability found in this typically inhomogeneous environment. Because of the nonlinear
345 response to precipitation, microwave-only precipitation retrievals are prone to the so-called beam-
346 filling problem (North and Polyak 1996): the satellite footprint or beam is not uniformly filled by
347 precipitation.

348 Ultimately, it is anticipated that NWP products with finer resolution and improved assimilation will
349 help resolve the sampling problem. The higher resolution fields released by ECMWF and other NWP
350 producers in support of the Year of Tropical Convection (e.g. Waliser and Moncrieff 2008) are a first
351 effort at this. However, routine, high-resolution NWP reanalyses with sufficient accuracy appear to be
352 decades in the future and will require considerable development of the basic flux physics (or flux
353 parameterizations) embedded in the model. We recommend the further development of high-latitude
354 reanalysis products, including the improvement of flux parameterizations, to address many of these
355 difficulties. However, we note that efforts to advance reanalyses and improve parameterizations are
356 likely to require better data.

357

358 **4. Summary: Key needs**

359 Obtaining improved estimates of high-latitude surface fluxes will require a multifaceted effort.
360 Coordinated sets of targeted observations are needed to refine flux parameterizations for high-latitude
361 conditions and to provide calibration and validation data. Given the difficult working conditions at
362 high latitudes and the vast region involved, satellites and numerical weather prediction models will
363 necessarily play a key role. This situation will likely require a multinational array of satellites designed

364 to provide good temporal and spatial sampling, carefully selected instrumentation, and improved
365 retrieval techniques aimed at minimizing errors in stress, air temperature, humidity, and cloud aerosol
366 properties.

367 Our recommendation is for the development of an expanded high-latitude observational network
368 that is sustained and optimized to improve physical parameterizations. New Arctic and Antarctic
369 reanalyses should be pursued, with goals of refining data retrieval algorithms and assessing different
370 models for boundary layers and fluxes in the presence of ice. Improving surface flux estimates in high-
371 latitude regions will require broad community involvement. Planning documents generated for
372 International Polar Year (IPY) and post-IPY activities have begun to articulate priorities (e.g., Dickson
373 2006; Rintoul et al. 2010). Some key ideas for improving fluxes emerged from discussions at a March
374 2010 workshop jointly organized by SeaFlux and the US CLIVAR Working Group on High Latitude
375 Surface Fluxes (summarized in sidebar #3). As a follow-up to the workshop and other post-IPY
376 discussion, it is critical that the community continue to seek consensus for plans to improve high-
377 latitude surface fluxes.

378

379 Acknowledgements: US CLIVAR provided logistical support and funding for the Working Group on
380 High Latitude Surface Fluxes. We also thank Ed Andreas, Shenfu Dong, Paul Hughes, Ryan Maue, and
381 E. Paul Oberlander for their contributions. CERES data used in Fig. 7 were downloaded from NASA
382 (<http://eosweb.larc.nasa.gov/GEWEX-RFA/>) and ISCCP data were obtained from the NASA Langley
383 Research Center EOSDIS. US CLIVAR and NASA supported the SeaFlux and High Latitude Surface
384 Fluxes Workshop.

385

386 **Sidebar 1: Primer: What is an air–sea flux?**

387 Air–sea fluxes represent the exchange of energy and material between the ocean and lower
388 atmosphere (Curry et al. 2004). They include the net fluxes of momentum (stress) from wind, energy
389 (downward and reflected shortwave radiation, downward and emitted longwave radiation, latent heat
390 flux, and sensible heat flux), and mass (Fig. 1). Mass fluxes encompass a broad number of variables
391 including moisture (precipitation and deposition, evaporation or sublimation, and runoff or ice melt)
392 and gases (e.g., CO₂) as well as atmospheric aerosols (solid or liquid particles), which can, for example,
393 supply salt to the atmosphere, provide chlorine that can contribute to ozone depletion, or deliver iron-
394 rich dust derived on land to the ocean, spurring biological growth.

395 Wind stress, sensible and latent heat fluxes, gas exchange, and evaporation are classified as
396 turbulent fluxes. These fluxes depend on nonlinear, co-varying terms, meaning that errors in
397 representing small-scale features can translate into significant errors even in large-scale averaged fields.
398 Depending upon the space and time scales being investigated (Fig. 3), these fluxes could be averaged
399 over a wide range of surface and meteorological conditions. Turbulent fluxes on the time scales of
400 intense storms (roughly one day) can be very large compared to long-term averages. Although
401 turbulent fluxes can be measured directly, they are typically parameterized (see Table 1) (e.g., Curry et
402 al. 2004). At high latitudes, low-level winds can be enhanced by orography and reduced friction over
403 some types of ice, leading to intense katabatic winds and low-level orographic jets, and consequently
404 strong air–sea momentum exchange along coastlines. Openings in the ice (i.e. leads and polynyas) can
405 lead to small-scale variations in air–sea turbulent heat fluxes, with strong heat exchange in open water
406 (Fig. 1). Small-scale ocean currents and eddies can also modify turbulent heat fluxes.

407 Radiative fluxes at the surface include downwelling and upwelling (reflected) shortwave radiation
408 (originating from the sun) as well as downwelling and upwelling longwave radiation (emitted by the
409 atmosphere and the surface, respectively.) Radiative fluxes exhibit unique characteristics at high-

410 latitude regions. For the downwelling shortwave, the major modulators at high latitudes are the low
411 solar angle and the polar night; the surface albedo that determines the reflected part varies strongly
412 between ice, snow, and water, and this is further complicated by the surface variability during melt
413 periods and by dust and carbonaceous aerosol deposition. Downwelling longwave radiation is
414 controlled largely by cloud cover, which is high at high latitudes, and by water vapor concentration,
415 which is small at high latitudes. The upwelling long-wave radiation depends on surface temperature,
416 which differs widely between the ice and the open water bodies and is not well known in areas with ice.
417 Furthermore, small changes in shortwave reflectivity and long-wave emissivity can alter the energy
418 budget sufficiently to cause substantial growth or melting of ice. All the radiative fluxes vary with
419 cloud cover and aerosol content, which in turn can depend on a number of regional factors such as
420 blowing snow and ice sublimation.

421 Net freshwater fluxes into the ocean are determined by the oceanic salinity flux, runoff (including
422 melting land ice). precipitation (P, which includes rain and snow), and evaporation (E) , the latter two
423 often viewed in the combined term of net precipitation, or $P-E$. The salinity flux is also proportional
424 to “ $P-E$ ” since salinity is the dilution of (conserved) salt by (non-conserved) freshwater. An important
425 factor for ocean freshwater and salinity balances in regions with sea ice is the fractionation of water
426 and salt in a process called brine rejection: sea ice is greatly depleted in salt, and most of the salt enters
427 the underlying seawater, where it increases the seawater density. When the sea ice melts, the resulting
428 seawater is significantly freshened and hence lighter. When sea ice, which can be thought of as
429 seawater of very low salinity, is transported from one region to another, an advective freshwater (and
430 salinity) flux between the regions arises. Ice and brine formation are modulated locally by the
431 intermixed areas of open water, organic slicks, new ice, existing bare ice, snow-covered ice, and melt
432 ponds; these interact with overlying regions of haze, low cloud, and clear sky, and are also affected by

433 sunlight reflection and gaseous deposition (e.g., of mercury). Subtle changes in heat or momentum
 434 fluxes cause, and respond to, rapid water phase change.

435

436 Table 1. Bulk formulas used to parameterize turbulent heat fluxes. The equations rely on differences
 437 between variables measured at known heights (e.g., 10 meters) above the ocean surface (e.g., \mathbf{U}_{10}) and
 438 those measured at the surface (e.g., \mathbf{U}_s). Terms include the friction velocity, \mathbf{u}_* , which is a complicated
 439 function of the wind shear ($\mathbf{U}_{10} - \mathbf{U}_s$), waves, and the atmospheric stratification; air density (ρ); and
 440 air–sea differences in temperature ($T_{10} - T_s$), humidity ($q_{10} - q_s$), or gas concentration ($G_{s,aq} - G_{10}/H$).
 441 Here θ_* and q_* are scaling parameters analogous to u_* , C_p is the specific heat of air, L_v is the latent heat
 442 of vaporization, and H is the Henry's law constant. The transfer coefficients (C_D , C_H , C_E , C_G), for
 443 momentum, specific heat, latent heat, and gas exchange, respectively, account for differences in scale
 444 and can include additional dependence on variability, \mathbf{u}_* , and atmospheric stability.

445

Momentum (wind stress)	$\boldsymbol{\tau} = \rho \mathbf{u}_* \mathbf{u}_* = \rho C_D (\mathbf{U}_{10} - \mathbf{U}_s) (\mathbf{U}_{10} - \mathbf{U}_s) $
Sensible heat flux	$Q_S = -\rho C_p \theta_* \mathbf{u}_* = \rho C_p C_H (T_{10} - T_s) (\mathbf{U}_{10} - \mathbf{U}_s) $
Evaporation	$E = -\rho q_* \mathbf{u}_* = \rho C_E (q_{10} - q_s) (\mathbf{U}_{10} - \mathbf{U}_s) $
Latent heat flux	$Q_L = -\rho L_v q_* \mathbf{u}_* \approx L_v E$
Air-sea gas exchange	$F_G = C_G (G_{s,aq} - G_{10}/H) (\mathbf{U}_{10} - \mathbf{U}_s) $

446

447

448 **Sidebar 2: Examples: Surfaces Fluxes From a Climate Research Perspective**

449 Surface flux products are widely used in the fields of oceanography, glaciology, sea ice dynamics, and

450 atmospheric dynamics. Science questions address time scales from hours to decades, resulting in a
451 diversity in related accuracy requirements. Here we provide a few examples.

452 *a. From a long-term climate change perspective*

453 Over the last few decades a number of aspects of the climate system have changed substantially. In
454 the ocean, observed long-term warming trends from 1993–2003 can be explained by a mean ocean heat
455 gain of just $0.86 \pm 0.12 \text{ W m}^{-2}$ (Hansen et al. 2005). For sea ice, a 1 W m^{-2} flux imbalance equates to a
456 10-cm ice melt in a year, which represents a significant fraction of the ice budget. Basin-scale changes
457 in ocean salinity associated with global change correspond to small changes in air–sea freshwater flux
458 on the order of 0.05 psu/decade (Boyer et al. 2005) concentrated in the top 200 m. This is equivalent to
459 a change in liquid P-E of 3 cm yr^{-1} . Similarly, North Atlantic freshwater flux anomalies sufficient to
460 slow deep convection (Curry and Mauritzen 2005) derive from river runoff and ice melt, and are
461 equivalent to P-E of almost 1 cm yr^{-1} over the area of the Arctic and North Atlantic. These climate
462 change signals of $O(1 \text{ W m}^{-2})$ for heat and $O(1 \text{ cm yr}^{-1})$ for freshwater are far below any currently
463 estimated observational accuracy globally or in polar regions, even in averaged estimates computed
464 from many independent samples. Hence, long-term changes in these fluxes are more effectively
465 diagnosed by observing the ocean temperature and salinity changes as integrators of heat and
466 freshwater fluxes (e.g., Hansen et al. 2005; Levitus et al. 2005; Boyer et al. 2005, 2007; Domingues et
467 al. 2007; Wunsch et al. 2007; Hosoda et al. 2009; Levitus et al. 2009; Durack and Wijffels, 2010).
468 Capabilities of current observing systems should not be a deterrent to efforts at improvement;
469 significant scientific gains could be made if the uncertainty in heat and freshwater flux estimates (as
470 crudely estimated by the spread in modern products) could be improved by an order of magnitude and
471 if available products were consistently released with high-quality uncertainty and bias information.

472 ***b. From an ocean circulation perspective***

473 The ocean circulation is driven primarily by wind stress curl patterns that deform sea level and
474 thermocline fields, and by heat and moisture fluxes that alter water density. Since the curl patterns are
475 caused in large part by zonal and meridional variations in the wind direction (e.g., easterly trades in the
476 tropics, westerly jet stream at midlatitudes), from the ocean circulation perspective it is necessary to
477 resolve not only the wind stress magnitude, but also its direction. Water density and hence circulation
478 are also modified by ventilation of the mixed layer through air–sea heat and freshwater fluxes. After the
479 water mass is subducted into the interior ocean, its properties remain relatively unchanged as it
480 circulates through the global ocean. The high-latitude ocean surface formation of ocean bottom water is
481 a critical component of the global ocean circulation. At high latitudes, surface cooling produces deeper
482 mixing and ventilation. Salinity becomes a major factor controlling density where temperatures
483 approach the freezing point. Thus, analysis of high-latitude ocean processes depends on accurate
484 surface heat and freshwater fluxes, including freshwater fluxes linked to ice formation, export, and
485 melt. For example, buoyancy gain by excess precipitation and buoyancy loss by ocean heat loss are
486 apparently of comparable importance in estimating Subantarctic Mode Water formation, which
487 dominates the upper ocean just north of the Antarctic Circumpolar Current (Cerovecki et al. 2011b).
488 Calculation of surface water mass transformation rates from air–sea fluxes requires accurate and
489 unbiased fluxes. Using the best available data products, Dong et al. (2007) found that the zonally
490 averaged imbalance can be 50 W m^{-2} , and locally, the upper-ocean heat balance can have a root-mean-
491 squared (RMS) misfit of more than 200 W m^{-2} at any given location, and 130 W m^{-2} in a global RMS-
492 averaged sense. Such large errors make it difficult to discern the details of the upper-ocean heat storage
493 and meridional overturning circulation. If RMS errors could be reduced to 10 W m^{-2} for weekly to
494 monthly time scales, the situation would clearly improve. Achieving such accuracy requires much

495 better sampling and a reduction in biases: strong winter storms account for much of the evaporation
496 (outside of western boundary currents; Scott 2011).

497 *c. From an atmospheric circulation perspective*

498 Winter land-surface flux anomalies can drive a quasi-stationary wave response that might reinforce
499 or attenuate climatological stationary waves propagating into the stratosphere, resulting in either a
500 negative or positive tropospheric annular mode response (e.g., Smith et al 2011). When considering
501 high-latitude surface fluxes due to opening or closing of sea-ice cover in particular, studies have shown
502 that certain “hotspots” for turbulent heat flux anomalies exhibit significant feedback between
503 atmospheric circulation patterns and modes of variability of sea ice. In the Northern Hemisphere, the
504 Barents Sea is such a location for the North Atlantic Oscillation (e.g., Strong et al 2009), the Bering Sea
505 for the West Pacific pattern (e.g., Matthewman and Magnusdottir 2011a). In the Southern Hemisphere,
506 no single pattern dominates in atmospheric variability and its interaction with sea-ice anomalies; rather
507 a superposition of the Pacific South America pattern and a quasi-stationary zonal wave train dominate
508 in interacting with sea ice anomalies (e.g., Yuan and Li 2008, Matthewman and Magnusdottir 2011b).
509 Turbulent energy fluxes resulting from the opening up of previously ice-covered areas of the Arctic are
510 especially large in boreal winter, averaging $O(50-70 \text{ W m}^{-2})$ (Alam and Curry 1997). The
511 understanding, detection, and modeling of these feedbacks would be improved if heat fluxes were
512 accurate to 10 W m^{-2} at 5–10-km spatial resolution and hourly time resolution. This would require
513 much more frequent sampling from satellites, increased accuracy in mean values, and reduced random
514 errors.

515 *d. From a sea ice mass balance perspective*

516 Arctic sea ice is a highly visible indicator of climate change. The range in recent and projected
517 future ice extent and volume from different models remains large, reflected in the surface energy fluxes
518 simulated both for the observational era and for future scenarios. Models are sensitive to small

519 perturbations in sea ice albedo (Bitz et al. 2006), and intermodel scatter in absorbed solar radiation, due
520 in part to differences in the surface albedo simulation, is a particular concern (Holland et al. 2010). Air–
521 sea heat fluxes can also play a role in determining ice thickness: Perovich et al. (2008) showed that
522 solar heating of open water in leads warms the upper ocean sufficiently to erode Arctic sea ice mass
523 from below. Ultimately, reduced ice thicknesses feed back on ocean–atmosphere processes by
524 changing the albedo (Brandt et al 2005) as well as the conductive and turbulent heat fluxes and emitted
525 (upward) surface longwave radiation through the ice.

526 The formation and presence of ice provokes a step-function change in radiative, heat, momentum,
527 and gas fluxes (e.g., Fig. 4). Ice formation and accumulation processes, which can include snow
528 refreezing (common in the Antarctic) and vertical migration of frazil ice and dissolution, erosion, and
529 break-up processes, remain highly complicated. These processes can occur on length scales too small
530 to be detected remotely or modeled explicitly with current technology. As stable multiyear ice
531 declines, annual ice processes and extent will dominate air–sea interaction and high-latitude fluxes.

532
533 **Sidebar 3: Recommendations for Improving High-Latitude Fluxes**

534 The myriad problems identified with high-latitude surface fluxes call for concerted efforts to identify
535 pathways toward improvement. With this in mind, the US CLIVAR Working Group on High Latitude
536 Surface Fluxes and the SeaFlux program together organized a workshop in Boulder, Colorado, 17-19
537 March 2010 (Bourassa et al. 2010b; Gille et al. 2010). The workshop attracted approximately 70
538 participants and included time for open discussion about priority strategies for improving flux
539 estimates. The issues summarized here represent topics for which community consensus seems clear.

- 540
- 541 1. *Acquire more in situ observations.* The dearth of observations in both high-wind open ocean
542 regimes and ice-covered regimes means that all additional flux-relevant data are desirable. This

543 includes standard meteorological data needed to compute fluxes from bulk parameterizations
544 (e.g., from the Shipboard Automated Meteorological and Oceanographic Systems (SAMOS)
545 program) as well as direct flux observations. A network of moorings (such as the Southern
546 Ocean Flux Station, deployed southwest of Tasmania in March 2010 as part of the Australian
547 Integrated Marine Observing System; Trull et al, 2010) would be desirable for capturing year-
548 round meteorological variability at fixed positions. Having large numbers of independent
549 samples is particularly important to reduce uncertainties in spatially and temporally averaged
550 flux estimates and in tuning satellite observations. Given the pitfalls associated with bulk
551 parameterizations, direct measurements of fluxes are also important. These are more likely to be
552 achieved from semiautonomous instrumentation that can be placed on board research vessels,
553 either during limited-duration process studies (such as GasEx) or as part of routine observations
554 from research vessels operating in high latitudes, which would allow light maintenance of the
555 instrumentation (such as the US NSF-sponsored Antarctic vessels or a NOAA-sponsored Arctic
556 ship). Aircraft observations are also important, particularly in marginal ice zones, though some
557 aircraft have had difficulties operating at low elevations in icy regimes; ultimately, unmanned
558 aerial vehicles (UAVs) may have a role in acquiring near surface atmospheric measurements.

559
560 Limited-duration process studies play an important role both in increasing the general inventory
561 of observations and also, more importantly, in helping to improve our understanding of physical
562 processes that govern fluxes. There is strong community consensus for an updated version of
563 the Surface Heat Budget of the Arctic Ocean (SHEBA) project and also for an Antarctic analog
564 to SHEBA aimed at capturing differences between Arctic and Antarctic sea ice zones

565
566 2. *Develop improved satellite flux observing capabilities.* Important as in situ measurements are,
567 ultimately the adverse conditions of high-latitude oceans, the vast size of the regions that need

568 to be observed, and the small spatial/temporal scales of the variability mean that we will need to
569 rely on satellite data to obtain a complete picture of air–sea fluxes. Satellite sensors are now
570 able to measure most of the relevant variables with some degree of accuracy, including ocean
571 wind or wind stress (scatterometry), sea surface temperature (infrared or microwave
572 radiometers), and near surface air temperature and humidity (atmospheric profiles such as the
573 Advanced Microwave Sounding Unit, AMSU, and the Atmospheric Infrared Sounder, AIRS).
574 The next stages underway are focused on developing improved retrieval algorithms that push
575 the limits of flux measurement capabilities from existing instruments. Ultimately, there is broad
576 interest in developing a coordinated system of satellite instruments for heat and momentum
577 fluxes. These could fly either on board a single satellite or on multiple satellites flying in
578 formation as a “Flux-Train,” analogous to the current series of atmospheric satellites known as
579 the A-Train. For time scales typical of the synoptic scale in the atmosphere, an accuracy of 5
580 Wm^{-2} in net energy fluxes is considered a desirable, albeit challenging, target for the combined
581 satellite and in situ observing system. Additional preliminary work will need to be completed to
582 determine the extent to which this is possible with current satellite technology.

583

584 3. *Make observations and flux products more accessible.* Along with the need for more
585 observations of high-latitude fluxes comes a parallel need to improve access to observations and
586 the flux products derived from them (such as NWP reanalyses). This involves a number of
587 issues that will benefit a broad range of user communities. Workshop participants noted that
588 data users sometimes select flux-related data products primarily on the basis of the time period
589 covered, the specific variables available, or even the convenience of finding data, without
590 considering the appropriateness of the dataset for a particular application. To address these
591 existing difficulties, first, flux-related data need to be easy to find. Although high-latitude data
592 are sparse, meteorological sensors have been installed on the Antarctic support vessels in recent

593 years, and a number of recent programs have collected observations in adverse high-latitude
594 conditions. Flux-related measurements from field programs, ships of opportunity, and satellites
595 need to be archived. Data collectors and product developers are encouraged to provide their
596 data to centers, where users can easily identify and cross-compare a wide range of
597 measurements and/or flux products that may be relevant for their work. More importantly, data
598 providers and data centers need to release flux-relevant data along with a full set of metadata
599 explaining the origins of the data and the inherent uncertainties.

600

601 4. *Encourage flux intercomparison.* Users of flux products often struggle to select a single flux
602 product from among the plethora of options derived using different methods, all with different
603 strengths and deficiencies. Given the lack of clear community consensus about how best to
604 determine fluxes, a better approach is to intercompare multiple products (e.g., Dong et al. 2007;
605 Cerovecki et al. 2011a). Data providers in particular recommended that users take time to
606 evaluate multiple flux products and to consider whether a particular flux product is suited for
607 various applications. In a multiproduct approach, the variability among different products can
608 serve as a crude measure of the robustness of results. While workshop participants suggested
609 that a multiproduct approach is nearly always appropriate, they were also enthusiastic about
610 establishing an organized effort to coordinate flux-product intercomparisons and synthesize the
611 results. For example, one suggestion was to develop a specific set of metrics (e.g., determining
612 the resolution of products, biases, and uncertainties) and techniques (e.g., power density
613 spectra) for evaluating flux data products that could be disseminated along with the data
614 themselves. A step beyond establishing metrics for flux evaluation would be a global effort to
615 improve surface flux estimates analogous to the effort of the Group for High-Resolution Sea
616 Surface Temperature (GHRSSST).

617 **References**

- 618 Alam, A. and J.A. Curry, 1997: Determination of surface turbulent fluxes over leads in arctic sea ice. *J.*
619 *Geophys. Res.*, **102**, 3331-3344.
- 620 Andreas, E. L. and K. A. Emanuel, 2001: Effects of sea spray on tropical cyclone intensity. *J. Atmos.*
621 *Sci.*, **58** (24), 3741–3751.
- 622 Andreas, E. L. and E. C. Monahan, 2000: The role of whitecap bubbles in air-sea heat and moisture
623 exchange. *J. Phys. Oceanogr.*, **30**, 433–442.
- 624 Andreas, E. L., P. O. G. Persson, J. E. Hare, 2008: A bulk turbulent air–sea flux algorithm for high-
625 wind, spray conditions. *J. Phys. Oceanogr.*, **38**, 1581–1596.
- 626 Berry, D. I., and E. C. Kent, 2011: Air–Sea fluxes from ICOADS: the construction of a new gridded
627 dataset with uncertainty estimates. *Int. J. Clim.*, **31**, 987-1001.
- 628 Bitz, C. M., P. R. Gent, R. A. Woodgate, M. M. Holland, and R. Lindsay, 2006: The influence of sea ice
629 on ocean heat uptake in response to increasing CO₂, *J. Climate*, **19**, 2437--2450.
- 630 Blanc, T. V., 1985: Variation of bulk-derived surface flux, stability, and roughness results due to the
631 use of different transfer coefficient schemes, *J. Phys. Oceanogr.*, **15**, 650-669.
- 632 Bourassa, M. A., 2006: Satellite-based observations of surface turbulent stress during severe weather,
633 Atmosphere - Ocean Interactions, Vol. 2., ed., W. Perrie, Wessex Institute of Technology Press,
634 Southampton, UK, 35 – 52 pp.
- 635 Bourassa, M. A., E. Rodriguez, and R. Gaston, 2010a: Summary of the 2008 and 2009 NASA Ocean
636 Vector Winds Science Team Meeting. *Bull. Amer. Meteor. Soc.*, **91**, doi:10.1175/2010BAMS2880.1.
- 637 Bourassa, M. A., S. Gille, D. L. Jackson, B. J. Roberts, and G. A. Wick, 2010b: Ocean Winds and
638 Turbulent Air-Sea Fluxes Inferred From Remote Sensing. *Oceanography*, **23**, 36-51.
- 639 Bourassa, M. A., et al., 2010c: Remotely sensed winds and wind stresses for marine forecasting and
640 ocean modeling. *Proceedings of the OceanObs'09: Sustained Ocean Observations and*

641 *Information for Society Conference (Vol. 2)*, Venice, Italy, eds. J. Hall, D.E. Harrison and D.
642 Stammer, ESA Publication WPP-306. doi:10.5270/OceanObs09.cwp.08

643 Boyer, T. P., J. I. Antonov, S. Levitus, and R. Locarnini, 2005: Linear trends of salinity for the world
644 ocean, 1955-1998. *Geophys. Res. Lett.*, **32**, L01604, doi:10.1029/2004GL021791.

645 Boyer, T., S. Levitus, J. Antonov, R. Locarnini, A. Mishonov, H. Garcia, and S. A. Josey, 2007:
646 Changes in freshwater content in the North Atlantic Ocean 1955-2006. *Geophys. Res. Lett.*, **34**,
647 L16603, doi:10.1029/2007GL030126.

648 Bradley, F, and C. Fairall, 2006: A guide to making climate quality meteorological and Flux
649 measurements at sea. NOAA Technical Memorandum OAR PSD-311, Department of Commerce,
650 109 pages.

651 Brandt, R. E., S. G. Warren, A. P. Worby, T. C. Grenfell, 2005: Surface albedo of the Antarctic
652 Sea Ice Zone. *J. Climate*, **18**, 3606–3622.

653 Cerovecki, I., L. D. Talley and M. R. Mazloff, 2011a: A comparison of Southern Ocean air-sea
654 buoyancy flux from an ocean state estimate with five other products. in press, *J. Climate*.

655 Cerovecki, I., L. Talley and M. Mazloff, 2011b: Subantarctic Mode Water and Antarctic Intermediate
656 Water Formation using a Walin framework. In preparation.

657 Chelton, Dudley B., Roland A. deSzoeko, Michael G. Schlax, Karim El Naggar, Nicolas Siwertz, 1998:
658 Geographical variability of the first baroclinic Rossby radius of deformation, *J. Phys. Oceanogr.*,
659 **28**, 433–460.

660 Christensen, J. H., and Coauthors, 2007: Regional climate change. *Climate Change 2007: The Physical
661 Science Basis*, S. Solomon et al., Eds., Cambridge University Press, 847-940.

662 Charlock, T. P., and T. L. Alberta, 1996: The CERES/ARM/GEWEX experiment (CAGEX) for the
663 retrieval of radiative fluxes with satellite data, *Bull. Am. Meteor. Soc.*, **77**, 2673-2683.

664 Comiso, J. C., C. L. Parkinson, R. Gersten, and L. Stock, 2008: Accelerated decline in the Arctic sea
665 ice cover, *Geophys. Res. Lett.*, **35**, L01703, doi:10.1029/2007GL031972.

666 Condron, A., G. R. Bigg, and I. A. Renfrew, 2008: Modeling the impact of polar mesocyclones on
667 ocean circulation. *J. Geophys. Res.*, **113**, doi:10.1029/2007JC004599 .

668 Curry, J. A., et al, 2004: SeaFlux, *Bull. Am. Meteor. Soc.*, **85**, 409-424.

669 Curry, J. A., J. L. Schramm, A. Alam, R. Reeder, T. E. Arbetter, and P. Guest, 2002: Evaluation of data
670 sets used to force sea ice models in the Arctic Ocean, *J. Geophys. Res.*, **107**, 8027,
671 doi:10.1029/2000JC000466.

672 Curry, R., and C. Mauritzen, 2005: Dilution of the Northern North Atlantic Ocean in Recent Decades,
673 *Science*, **308**, 1772–1774.

674 Dickson, B., 2006: The integrated Arctic Ocean Observing System (iAOOS): an AOSB-CliC
675 Observing Plan for the International Polar Year, *Oceanologia*, **48**, 5-21.

676 Domingues, C. M., J. A. Church, N. J. White, P. J. Gleckler, S. E. Wijffels, P. M. Barker, and J. R.
677 Dunn, 2008: Improved estimates of upper-ocean warming and multi-decadal sea-level rise. *Nature*,
678 **453**, 1090-1096.

679 Dong, S., S. T. Gille, and J. Sprintall, 2007: An assessment of the Southern Ocean mixed-layer heat
680 budget, *J. Climate*, **20**, 4425-4442.

681 Dong, S., S. T. Gille, J. Sprintall, and E. J. Fetzer, 2010: Assessing the potential of the Atmospheric
682 Infrared Sounder (AIRS) surface temperature and relative humidity in turbulent heat flux estimates
683 in the Southern Ocean, *J. Geophys. Res.*, **115**, C05013, doi:10.1029/2009JC005542.

684 Donlon, C., et al., 2007: The Global Ocean Data Assimilation Experiment High-resolution Sea Surface
685 Temperature Pilot Project. *Bull. Amer. Meteorol. Soc.*, **88**, 1197–1213.

686 Durack, P. J., and S. E. Wijffels, 2010: Fifty-year trends in global ocean salinities and their relationship
687 to broad- scale warming. *J. Clim.*, **23**, 4342-4362.

688 Engelen, R. J., E. Andersson, F. Chevallier, A. Hollingsworth, M. Matricardi, A. P. McNally, J.-N.
689 Thépaut, and P. D. Watts, 2004: Estimating atmospheric CO₂ from advanced infrared satellite
690 radiances within an operational 4D-Var data assimilation system: Methodology and first results. *J.*
691 *Geophys. Res.*, **109** (D19), D19 309, doi:10.1029/2004JD004777.

692 Engelen, R. J. and A. P. McNally, 2005: Estimating atmospheric CO₂ from advanced infrared satellite
693 radiances within an operational four-dimensional variational (4D-Var) data assimilation system:
694 Results and validation. *J. Geophys. Res.*, **110** (D18), D18 305, doi:10.1029/2005JD005982.

695 Engelen, R. J. and G. L. Stephens, 2004: Information content of infrared satellite sounding
696 measurements with respect to CO₂. *J. Appl. Meteor.*, **43** (2), 373–378.

697 Fairall, C. W., E. F. Bradley, D. P. Rogers, J. B. Edson, and G. S. Young, 1996: Bulk parameterization
698 of air-sea fluxes for TOGA COARE. *J. Geophys. Res.*, **101**, 3747-3767.

699 Fairall, C. W., M. Banner, W. Peirson, R. P. Morison, and W. Asher, 2009: Investigation of the physical
700 scaling of sea spray spume droplet production. *J. Geophys., Res.*, **114**, C10001,
701 doi:10.1029/2008JC004918.

702 Gille, S. T., 2002: Warming of the Southern Ocean since the 1950s, *Science*, **295**, 1275-1277.

703 Gille, S., M. A. Bourassa, and C. A. Clayson, 2010: Improving observations of high-latitude fluxes
704 between atmosphere, ocean, and ice, *EOS*, **91**, 307.

705 Gruber, A. and V. Levizzani, 2008: Assessment of global precipitation products: A project of the
706 World Climate Research Programme Global Energy and Water Cycle Experiment (GEWEX)
707 Radiation Panel, World Climate Research Programme, Geneva, WCRP-128, WMO/TD-No. 1430.

708 Guest, P. S. 1998: Surface longwave radiation conditions in the eastern Weddell Sea during winter, *J.*
709 *Geophys. Res.*, **103**(C13), 30,761–30,771.

710 Gulev, S. K., T. Jung, and E. Ruprecht, 2007a: Estimation of the impact of sampling errors in the VOS
711 observations on air-sea fluxes. Part I. Uncertainties in climate means. *J. Climate*, **20**, 279-301.

712 Gulev, S. K., T. Jung, and E. Ruprecht, 2007b: Estimation of the impact of sampling errors in the VOS
713 observations on air-sea fluxes. Part II. Impact on trends and interannual variability. *J. Climate*, **20**,
714 302-315.

715 Hansen, J., L. Nazarenko, R. Ruedy, M. Sato, J. Willis, A. Del Genio, D. Koch, A. Lacis, K. Lo, S.
716 Menon, T. Novakov, J. Perlwitz, G. Russell, G. A. Schmidt, N. Tausnev, 2005. Earth's energy
717 imbalance: Confirmation and implications, *Science*, **308**, doi: 10.1126/science.1110252.

718 Ho, D. T., F. Veron, E. Harrison, L. F. Bliven, N. Scott, Nicholas, W. R. McGillis, 2007: The combined
719 effect of rain and wind on air-water gas exchange: A feasibility study, *J. Mar. Sys.*, **66**, 150-160.

720 Holland. M. M., M. C. Serreze and J. Stroeve, 2010: The sea ice mass budget of the Arctic and its
721 future change as simulated by coupled climate models, *Climate Dynamics*, **34**, 185-200

722 Hosoda, S., T. Suga, N. Shikama, and K. Mizuno, 2009: Global surface layer salinity change detected
723 by Argo and its implication for hydrological cycle intensification. *J. Oceanogr.*, **65**, 579-586.

724 Huffman, G. J. et al., 1997: The Global Precipitation Climatology Project (GPCP) combined
725 precipitation data set, *Bull. Amer. Meteor. Soc.*, **78**, 5-20.

726 Jackson, D. L., G. A. Wick, and J. J. Bates, 2006: Near-surface retrieval of air temperature and specific
727 humidity using multisensor microwave satellite observations, *J. Geophys. Res.*, **111**, D10306,
728 doi:10.1029/2005JD006431.

729 Jackson, D.L., G.A. Wick, and F.R. Robertson, 2009: Improved multi-sensor approach to satellite-
730 retrieved near-surface specific humidity observations. *J. Geophys. Res.* **114(D)**16303,
731 doi:10.1029/2008JD011341.

732 Jackson, D.L., and G.A. Wick, 2010: Near-surface air temperature retrieval derived from AMSU-A and
733 sea surface temperature observations. *J. Atmos. Ocean. Tech.*, **27**, 1769–1776.

734 Jiang, C., S. T. Gille, J. Sprintall, K. Yoshimura, and M. Kanamitsu, 2011: Spatial variation in turbulent
735 heat fluxes in Drake Passage, in press *J. Climate*.

736 Kahn, R. A., B. J. Gaitley, J. V. Martonchik, D. J. Diner, K. A. Crean, and B. Holben (2005). Multiangle
737 Imaging Spectroradiometer (MISR) global aerosol optical depth validation based on 2 years of
738 coincident Aerosol Robotic Network (AERONET) observations. *J. Geophys. Res.*, **110**, D10S04,
739 doi:10.1029/2004JD004706.

740 Karcher, M. J., R. Gerdes, F. Kauker, and C. Köberle, 2003: Arctic warming: Evolution and spreading
741 of the 1990s warm event in the Nordic seas and the Arctic Ocean, *J. Geophys. Res.*, **108**(C2),
742 3034, doi:10.1029/2001JC001265.

743 Key, J. R., Silcox, R. A. and Stone, R. S., 1996: Evaluation of surface radiative flux parameterizations
744 for use in sea ice models. *J. Geophys. Res.* **101**, 3839–3849.

745 König-Langlo, G. and E. Augstein, 1994: Parameterization of the downward long-wave radiation at the
746 Earth's surface in polar regions. *Meteorol. Z.* **3**, 343–347.

747 Kwok, R. and N. Untersteiner, 2011: The thinning of Arctic sea ice, *Phys. Today*, **64**, 44-49.

748 Levitus, S., J. Antonov and T. Boyer, 2005: Warming of the world ocean, 1955-2003, *Geophys. Res.*
749 *Lett.*, **32**, L02604, doi:10.1029/2004GL021592.

750 Levitus, S., J. I. Antonov, T. P. Boyer, R. A. Locarnini, H. E. Garcia, and A. V. Mishonov, 2009: Global
751 ocean heat content 1955-2008 in light of recently revealed instrumentation problems. *Geophys.*
752 *Res. Lett.*, **36**, L07608, doi:10.1029/2008GL037155.

753 Lewis, E.R., and E.W. Schwartz, 2004: Sea Salt Aerosol Production: Mechanisms, Methods,
754 Measurements and Models - A Critical Review. *Geophys. Monogr. Ser.*, Vol. 152, 413 pp, AGU,
755 Washington, DC.

756 Liu, J. P., J. A. Curry, W. B. Rossow, J. R. Key, and X. Wang, 2005: Comparison of surface radiative
757 flux data sets over the Arctic Ocean. *J. Geophys. Res.*, **110**, C02015, doi: 10.1029/2004JC002381,
758 1-13.

759 Lubin, D. and A. M. Vogelmann, 2006: A climatologically significant aerosol longwave indirect effect
760 in the Arctic, *Nature*, **439**, 453-456.

761 Makshtas, A. P., E. L. Andreas, P. N. Svyashchennikov, V. F. Timachev, 1999: Accounting for clouds in
762 sea ice models, *Atmos. Res.*, **52**, 77-113.

763 Martz, T. R., M. D. DeGrandpre, P. G. Strutton, W. R. McGillis, and W. M. Drennan, 2009: Sea surface
764 pCO₂ and carbon export during the Labrador Sea spring-summer bloom: An in situ mass balance
765 approach, *J. Geophys. Res.*, **114**, C09008, doi:10.1029/2008JC005060.

766 Matthewman, N. J., and G. Magnusdottir, 2011a: Observed interaction between Pacific sea ice
767 anomalies and the Western Pacific pattern on intraseasonal time scales. *J. Climate*, **24**, 5031-5042.

768 Matthewman, N. J., and G. Magnusdottir, 2011b: Clarifying ambiguity in intraseasonal Southern
769 Hemisphere climate modes during austral winter. *J. Geophys. Res.*, accepted.

770 Michalsky, J., E. Dutton, M. Rubes, D. Nelson, T. Stoffel, M. Wesley, M. Splitt, and J. DeLuisi, 1999:
771 Optimal measurement of surface shortwave irradiance using current instrumentation. *J. Atmos.*
772 *Oceanic Technol.*, **16**, 55–69.

773 Moore, G. W. K., R. S. Pickart, and I. A. Renfrew, 2008: Buoy observations from the windiest location
774 in the world ocean, Cape Farewell, Greenland, *Geophys. Res. Lett.*, **35**, L18802,
775 doi:10.1029/2008GL034845.

776 Mueller, J., and F. Veron, 2009: A nonlinear formulation of the bulk surface stress over the ocean
777 through a simple feedback mechanism. *Bound.-Layer Meteorol.*, **130**, 117-134.

778 North, G. R., and I. Polyak, 1996: Spatial correlation of beam-filling error in microwave rain-rate
779 retrievals. *J. Atmos. Oceanic Technol.*, **13**, 1101–1106.

780 Nussbaumer, E. A. and R. T. Pinker, 2011: Estimating surface longwave radiative fluxes from satellites
781 utilizing artificial neural networks, *J. Geophys. Res.*, in preparation.

782 Ohmura, A., et al., 1998: Baseline Surface Radiation Network (BSRN/WRMC), a new precision
783 radiometry for climate research, *Bull. Am. Meteorol. Soc.*, **79**, 2115– 2136.

784 Perovich, D. K., E. L. Andreas, J. A. Curry, H. Eiken, C. W. Fairall, T. C. Grenfell, P. S. Guest, J.
785 Intrieri, D. Kadko, R. W. Lindsay, M. G. McPhee, J. Morison, R. E. Moritz, C. A. Paulson, W. S.

786 Pegau, P. O. G. Persson, R. Pinkel, J. A. Richter-Menge, T. Stanton, H. Stern, M. Sturm, W. B.
787 Tucker III, and T. Uttal, 1999: Year on ice gives climate insights. *Eos Trans. AGU*, **80**, 481, 485-
788 486.

789 Perovich, D. K., J. A. Richter-Menge, K. F. Jones, and B. Light, 2008: Sunlight, water, and ice:
790 Extreme Arctic sea ice melt during the summer of 2007, *Geophys. Res. Lett.*, **35**, L11501,
791 doi:10.1029/2008GL034007.

792 Petersen, G.N. and I.A. Renfrew, 2009: Aircraft-based observations of air-sea fluxes over Denmark
793 Strait and the Irminger Sea during high wind speed conditions, *Quarterly J. Royal Meteorol. Soc.*,
794 **135**, 2030-2045.

795 Pietroni, I., P. Anderson, S. Argentini, and J. King, 2008: Long wave radiation behaviour at Halley and
796 Concordia stations, Antarctica. SRef-ID: 1607-7962/gra/EGU2008-A-03254 EGU General
797 Assembly 2008.

798 Pinker, R. T., R. Frouin, and Z. Li, 1995: A review of satellite methods to derive surface shortwave
799 irradiance, *Rem. Sens. Env.*, **51**, 108-124.

800 Purkey, S. G., and G. C. Johnson. 2010: Warming of global abyssal and deep Southern Ocean waters
801 Between the 1990s and 2000s: Contributions to global heat and sea level rise budgets. *J. Climate*,
802 **23**, 6336-6351, doi:10.1175/2010JCLI3682.1.

803 Randall, D. A., et al., 2007: Climate models and their evaluation. *Climate Change 2007: The Physical
804 Science Basis*, S. Solomon et al., Eds., Cambridge University Press, 589-662.

805 Remer, L. A. , Y. J. Kaufman, D. Tanre, S. Mattoo, D. A. Chu, J. V. Martins, R. R. Li, C. Ichoku, R. C.
806 Levy, R. G. Kleidman, T. F. Eck, E. Vermote, and B. N. Holben, 2005: The MODIS aerosol
807 algorithm, products, and validation, *J. Atmos. Sci.*, **62**(4), 947-973.

808 Renfrew, I.A., G.W.K. Moore, P.S. Guest, and K. Bumke, 2002: A comparison of surface-layer and
809 surface turbulent-flux observations over the Labrador Sea with ECMWF analyses and NCEP
810 reanalyses, *J. Phys. Oceanogr.*, **32**, 383-400.

811 Renfrew, I.A., et al., 2008: The Greenland Flow Distortion experiment, *Bull. Amer. Meteorol. Soc.*, **89**,
812 1307-1324.

813 Rignot, E., G. Casassa, P. Gogineni, W. Krabill, A. Rivera, and R. Thomas, 2004: Accelerated ice
814 discharge from the Antarctic Peninsula following the collapse of Larsen B ice shelf, *Geophys. Res.*
815 *Lett.*, **31**, L18401, doi:10.1029/2004GL020697.

816 Rintoul, S. et al., 2010: "Southern Ocean Observing System (SOOS): Rationale and Strategy for
817 Sustained Observations of the Southern Ocean" in *Proceedings of OceanObs'09: Sustained Ocean*
818 *Observations and Information for Society (Vol. 2)*, Venice, Italy, 21-25 September 2009, Hall, J.,
819 Harrison D.E. & Stammer, D., Eds., ESA Publication WPP-306.

820 Risien, C. M., and D. B. Chelton, 2008: A global climatology of surface wind and wind stress fields
821 from eight years of QuikSCAT scatterometer data. *J. Phys. Oceanogr.*, **38**, 2379-2413.

822 Roberts, J. B., C. A. Clayson, F. R. Robertson, and D. Jackson, 2010: Predicting near-surface
823 characteristics from SSM/I using neural networks with a first guess approach. *J. Geophys. Res.*,
824 **115**, D19113, doi:10.1029/2009JD013099

825 Sapiano, M. R. P., 2010: An evaluation of high resolution precipitation products at low resolution, *Intl.*
826 *J. Climatology*, **30** 1416–1422.

827 Scambos, T., H. A. Fricker, C.-C. Liu, J. Bohlander, J. Fastook, A. Sargent, R. Massom and A.-M. Wu,
828 2009: Ice shelf disintegration by plate bending and hydro-fracture: Satellite observations and
829 model results of the 2008 Wilkins ice shelf break-ups, *Earth Planetary Science Lett.* **280**, 51-60.

830 Schaaf CB, Gao F, Strahler AH, et al., 2002: First operational BRDF, albedo nadir reflectance products
831 from MODIS, *Rem. Sens. Env.*, **83**, 135-148.

832 Schlax, M. G., D. B. Chelton and M. H. Freilich, 2001: Sampling errors in wind fields constructed from
833 single and tandem scatterometer datasets. *J. Atmos. Oceanic Tech.*, **18**, 1014-1036.

834 Schemtz, J., 1989: Towards a surface radiation climatology: retrieval of downward irradiance from
835 satellites. *Atmos. Res.*, **23**, 287-321.

836 Schmetz, J., 1991: Retrieval of surface radiation fluxes from satellite data, *Dyn. Atmos. Ocean.* **16** (1-
837 2), 61-72.

838 Schmetz, J., 1993: On the relationship between solar net radiative fluxes at the top of the atmosphere
839 and at the surface, *J. Atmos. Sci.*, **50** 1122–1132.

840 Scott, J. P., 2011: An intercomparison of numerically modeled flux data and satellite-derived flux data
841 for warm seclusions. MS Thesis, Florida State University, Tallahassee, FL 32306.
842 <http://etd.lib.fsu.edu/theses/available/etd-05242011-121615/>

843 Serreze, M. C. and C. M. Hurst, 2000: Representation of mean Arctic precipitation from NCEP-NCAR
844 and ERA Reanalyses, *J. Climate*, **13**, 182-201.

845 Serreze, M. C., A. P. Barrett, and F. Lo, 2005: Northern high-latitude precipitation as depicted in
846 atmospheric reanalyses and satellite retrievals, *Mon. Wea. Rev.*, **133**, 3407-3430.

847 Shi, Y, and C. N. Long, 2004: Techniques and methods used to determine the best estimate of total
848 downwelling shortwave radiation. In *Proc. of the Fourteenth Atmospheric Radiation Measurement*
849 *(ARM) Science Team Meeting*, Albuquerque, New Mexico, March 22-26, 2004, 9 pp. U.S.
850 Department of Energy, Washington, DC.

851 Smith, K. L., P. J. Kushner, and J. Cohen, 2011: The role of linear interference in northern annular
852 mode variability associated with Eurasian snow cover extent. *J. Climate*, in press.

853 Smith, S., P. Hughes, and M. Bourassa, 2010: A comparison of nine monthly air-sea flux products.
854 *Internat. J. Clim.*, **30**, 26 pp., DOI: 10.1002/joc.2225.

855 Sorteberg, A., V. Kattsov, J. E. Walsh, and T. Pavlova, 2007: The Arctic surface energy budget as
856 simulated with the IPCC AR4 AOGCMs, *Climate Dynamics*, **29**, 131-156.

857 Stackhouse, P. W., Jr., et al., 2004: 12-year Surface Radiation Budget Data Set, *GEWEX News*, **14**, 10–
858 12.

859 Strong, C., G. Magnusdottir and H. Stern, 2009: Observed feedback between winter sea ice and the
860 North Atlantic Oscillation. *J. Climate*, **22**, 6021-6032.

861 Strow, L. L. and S. E. Hannon, 2009: A 4-year zonal climatology of lower tropospheric CO₂ derived
862 from ocean-only atmospheric infrared sounder observations. *J. Geophys. Res.*, **113**, D18 302,
863 doi:10.1029/2007JD009713.

864 Trull, T. W., E. Schulz, S. G. Bray, L. Pender, D. McLaughlan, B. Tilbrook, M. Rosenberg, and T.
865 Lynch, 2010: The Australian Integrated Marine Observing System Southern Ocean Time Series
866 facility, *OCEANS 2010 IEEE - Sydney*, pp.1-7, 24-27 May 2010 doi:
867 10.1109/OCEANSSYD.2010.5603514.

868 Turner, D. D. and E. J. Mlawer, 2010: Radiative heating in underexplored bands campaigns (RHUBC).
869 *Bull. Amer. Meteor. Soc.*, **91**, 911–923.

870 Vancoppenolle, M., R. Timmermann, S.F. Ackley, T. Fichefet, H. Goosse, P. Heil, J. Lieser, K.C.
871 Leonard, M. Nicolaus, T. Papakyriakou and J.-L. Tison, 2011. Assessment of radiation forcing data
872 sets for large-scale sea ice models in the Southern Ocean. *Deep-Sea Res.*, **58**, 1237-1249.

873 Waliser, D. and M. Moncrieff, 2008: The YOTC Science Plan, World Meteorological Organization
874 Report WMO/TP No. 1452. WCRP No. 130.

875 Wang, H., and R. T. Pinker, 2009: Shortwave radiative fluxes from MODIS: Model development and
876 implementation, *J. Geophys. Res.*, **114**, D20201, doi:10.1029/2008JD010442.

877 Wanninkhof, R., W. E. Asher, D. T. Ho, C. Sweeney, and W. R. McGillis, 2009: Advances in
878 Quantifying Air-Sea Gas Exchange and Environmental Forcing, *Ann. Rev. Mar. Sci.* **1**, 213-244.

879 WCRP, 2000: Intercomparison and validation of ocean-atmosphere energy flux fields. Working Group
880 on air-sea fluxes, Technical report of the World Climate Research Programme, WCRP-112, 303 pp.

881 Weissman, D. E., and M. A. Bourassa, 2011: The influence of rainfall on scatterometer backscatter
882 within tropical cyclone environments – implications on parameterization of sea surface stress. *Trans.*
883 *Geosci. Remote Sens.* (in press).

884 Whitlock, C., T. Charlock, W. Staylor, R. Pinker, I. Laszlo, A. Ohmura, H. Gilgen, T. Konzelman, R.
885 DiPasquale, C. Moats, S. LeCroy, and N. Ritchey, 1995: First 40 Global WCRP Shortwave Surface
886 Radiation Budget Dataset, *Bull. Amer. Meteor. Soc.*, **76**, 905–922.

887 Wielicki, B. A., et al., 1995: Mission to Planet Earth-role of clouds and radiation in climate. *Bull.*
888 *Amer. Meteor. Soc* **76**, 2125-2153.

889 Wielicki, B. A., B. R. Barkstrom, E. F. Harrison, R. B. Lee III, G. L. Smith, and J. E. Cooper, 1996:
890 Clouds and the Earth's Radiant Energy System (CERES): An Earth Observing System Experiment,
891 *Bull. Amer. Meteor. Soc.*, **77**, 853-868.

892 Wilson, E. L., E. M. Georgieva and W. S. Heaps, 2007: Development of a Fabry–Perot interferometer
893 for ultra-precise measurements of column CO₂. *Meas. Sci. Technol.* **18** 1495, doi:10.1088/0957-
894 0233/18/5/040.

895 Woolf, D.K., 2005: Parameterization of gas transfer velocities and sea-state-dependent wave breaking.
896 *Tellus B*, **57**, 87-94.

897 Wunsch, C., R. M. Ponte, and P. Heimbach, 2007. Decadal trends in sea level patterns: 1993-2004, *J.*
898 *Climate*, **20**, 5889-5911.

899 Yang, D., 1999: An improved precipitation climatology for the Arctic Ocean, *Geophys. Res. Lett.*, **26**,
900 1525-1528.

901 Yuan, X, and C. Li, 2008: Climate modes in southern high latitudes and their impacts on Antarctic sea
902 ice. *J. Geophys. Res.*, **113**, C06S91, doi:10.1029/2006JC004067.

903 Xie, P. and P. A. Arkin, 1997: Global precipitation: A 17-year monthly analysis based on gauge
904 observations, satellite estimates and numerical model output, *Bull. Amer. Meteor. Soc.*, **78**, 2539-
905 2558.

906 Zhang, Y. C., W. B. Rossow, A. A. Lacis, V. Oinas, and M. I. Mishchenko, 2004: Calculation of
907 radiative fluxes from the surface to top of atmosphere based on ISCCP and other global data sets:

908 Refinements of the radiative transfer model and the input data, *J. Geophys. Res.*, **109**, D19105,
909 doi:10.1029/2003JD004457.

910 Zhao, W., W. R. Kuhn, and S. R. Drayson,1994: The significance of detailed structure in the boundary
911 layer to thermal radiation at the surface in climate models. *Geophys. Res. Lett.*, **21**, 1631-1634.

912

913

914

915 Figure Captions

916

917 **Figure 1.** Schematic of surface fluxes and related processes for high latitudes. Radiative fluxes are
918 both shortwave (SW) and longwave (LW). Surface turbulent fluxes are stress, sensible heat (SHF), and
919 latent heat (LHF). Ocean surface moisture fluxes are precipitation and evaporation (proportional to
920 LHF). Processes specific to high-latitude regimes can modify fluxes. These include strong katabatic
921 winds, effects due to ice cover and small-scale open patches of water associated with leads and
922 polynyas, air-sea temperature differences that vary on the scale of eddies and fronts (i.e., on the scale of
923 the oceanic Rossby radius, which can be short at high latitudes), and enhanced fresh water input
924 associated with blowing snow.

925

926 **Figure 2.** Frequency of winds exceeding 25m/s for the QuikSCAT observations from July 1999
927 through June 2009, based on Remote Sensing Systems' Ku2001 algorithm. Statistics are computed by
928 averaging vector winds from the original satellite swath measurements into 0.25° by 0.25° bins.
929 Northern Hemisphere extreme winds are associated with topography (e.g. around Greenland, see
930 Renfrew et al. 2008) and western boundary currents and occur in boreal winter; Southern Hemisphere
931 events are more widespread and occur year around. Locations with less than approximately 51% of
932 possible observations are plotted as white, thereby excluding some regions with too much seasonal ice.

933

934 **Figure 3.** Spatial and temporal scales for high-latitude processes and the recommended accuracy of
935 related surface fluxes. These accuracies are estimates from a wide range of scientists working on
936 related processes. The accuracy requirements are difficult to determine or validate, as the modeling and
937 observational errors, as well as the validity of assumptions, in current estimates are not sufficiently well
938 understood to quantify requirements.

939

940

941 **Figure 4.** Boundary-layer observations of a cold-air outbreak off the east coast of Greenland during an
942 instrumented aircraft flight on 5 March 2007, as a function of distance from the coast. Panels show
943 (top) 2-m temperature (red) and sea surface temperature (blue); (middle) 10-meter wind speed; and
944 (bottom) surface sensible (red) and latent (blue) heat fluxes calculated using the eddy covariance
945 method (taken from Petersen and Renfrew 2009) as a function of distance. The observations are
946 averaged into 12-km runs (circles). Interpolated estimates from ECMWF operational analyses (solid
947 line) and the much coarser resolution NCEP global reanalyses (dashed line) are also plotted. The plots
948 show a rapid warming from over the sea ice zone (0–30 km) off shore and a jump in wind speed and
949 observed heat fluxes across the ice edge.

950

951 **Figure 5.** Comparison of oceanic sensible (top) and latent (bottom) heat fluxes from readily available
952 products: NCEP2 (blue), JMA (green), ERA40 (purple), IFREMER (red), and HOAPS (cyan). Each
953 box shows zonally averaged (0 through 360 degrees) monthly fluxes for the 5th, 25th, 50th, 75th, or 95th
954 percentiles. The period for comparison (for which all products are available) is March 1992 through
955 December 2000. Clearly there are very large differences in the distribution of fluxes. Note that the
956 range of fluxes (x -axis) is not constant, with the range for the 95th percentile being about 4 times the
957 range for the 5th percentile. Furthermore, there is a great deal of regional surface flux variability in all
958 high-latitude seas: product differences are greater on smaller spatial and temporal scales. Details about
959 the data, parameterizations and assumptions used to develop these products are given in Smith et al.
960 (2010).

961

962

963 **Figure 6.** The 10-m neutral turbulent transfer coefficients (C_{d10n} , C_{E10n} , C_{H10n}) and the CO₂ transfer
964 velocity ($K_{660} = C_G |(U_{10} - U_s)|$) as a function of 10-m neutral wind speed from direct surface-based

965 observations: drag coefficient (top), heat transfer coefficients (middle), and CO₂ transfer coefficient
966 (bottom). A percentage error in the transfer coefficient results in a similar percentage error in the flux:
967 differences in parameterizations are greatest at low and high wind speeds. The black line is the mean of
968 the data sets; the error bars are statistical estimates of the uncertainty in the mean. The
969 parameterizations shown in the top two panels are COARE algorithm (red), NCEP reanalysis (green),
970 ECMWF (blue), Large and Yeager (magenta). Symbols on the upper two panels are circle – U.
971 Connecticut (FLIP, Martha’s Vineyard Observatory, and moored buoys), diamond – U. Miami (ASIS
972 spar buoy), and square – NOAA/ESRL (ships). The gas transfer coefficient parameterizations shown in
973 the bottom panel are– McGillis et al. 2001 (blue dashed line), NOAA/COARE CO₂ (red dashed line).
974 CO₂ panel symbols are circle – GASEX98, square – GASEX01, diamond – GASEX08 (data courtesy J.
975 Edson, W. McGillis).

976

977 **Figure 7.** Comparison of the zonal mean downwelling shortwave flux products averaged for two July
978 months (2003 and 2004) from four products: CERES (Wielicki et al., 1996); ISCCP-FD (Zhang et al.,
979 2004); UMD/V3.3.3: and MODIS (Wang and Pinker, 2009). Note the relatively large disagreement in
980 the Northern Hemisphere and particularly the Arctic latitudes.

981

982

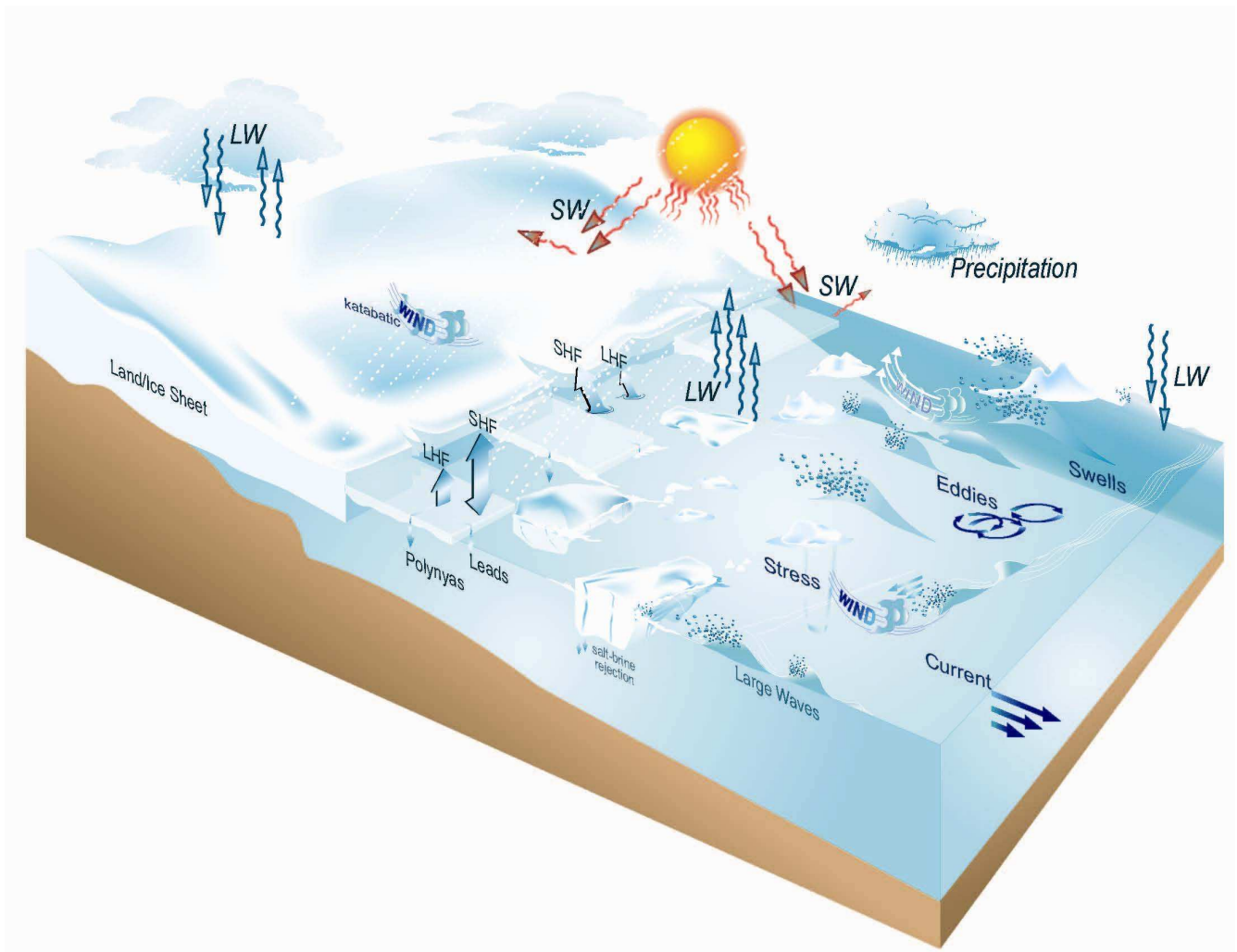
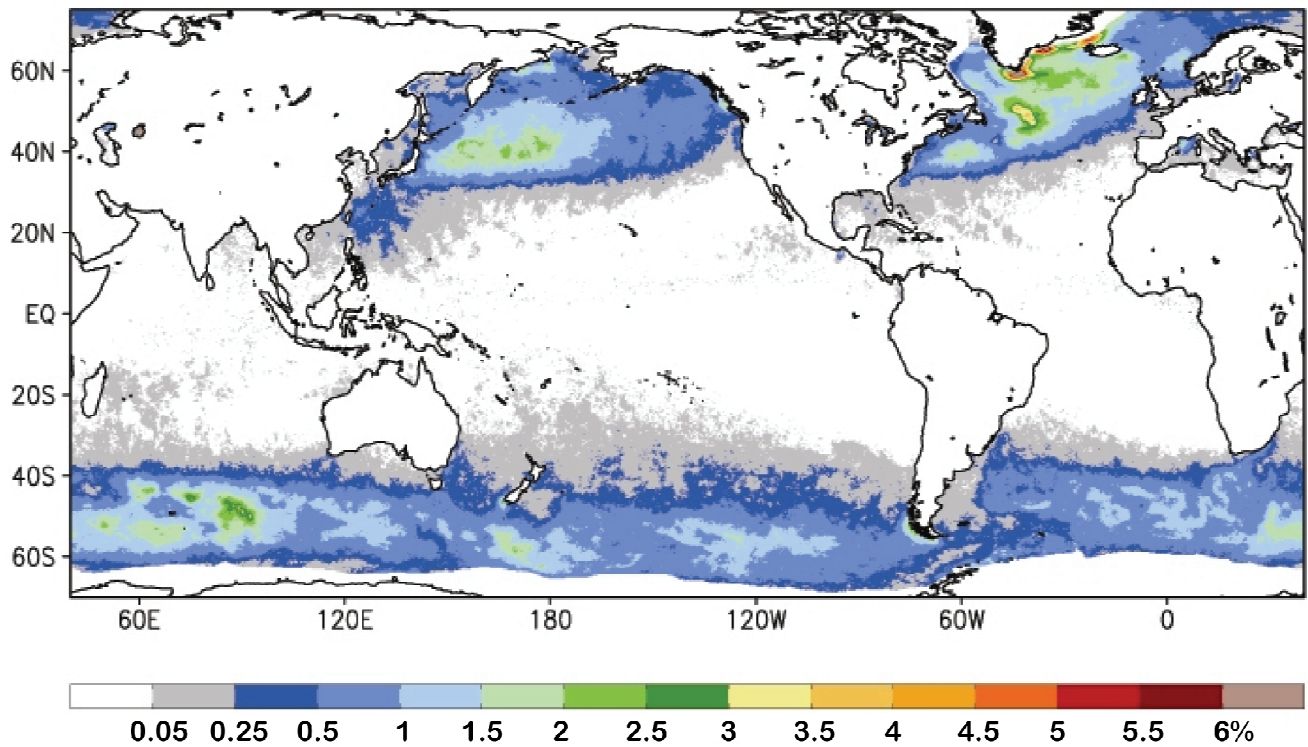


Figure 1. Schematic of surface fluxes and related processes for high latitudes. Radiative fluxes are both shortwave (SW) and longwave (LW). Surface turbulent fluxes are stress, sensible heat (SHF) and latent heat (LHF). Ocean surface moisture fluxes are precipitation and evaporation (proportional to LHF). Processes specific to high-latitude regimes can modify fluxes. These include strong katabatic winds, effects due to ice cover and small-scale open patches of water associated with leads and polynyas, air-sea temperature differences that vary on the scale of eddies and fronts (i.e., on the scale of the oceanic Rossby radius, which can be short at high latitudes), and enhanced fresh water input associated with blowing snow.



995

996

997

998

999

1000

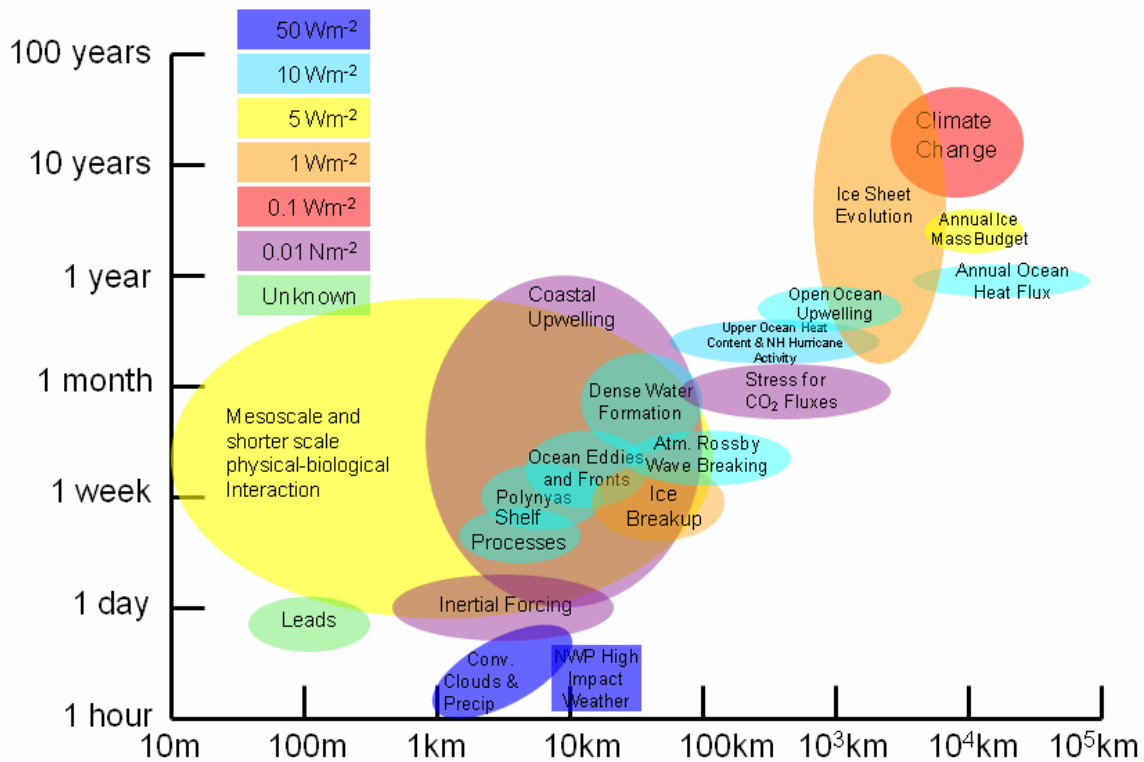
1001

1002

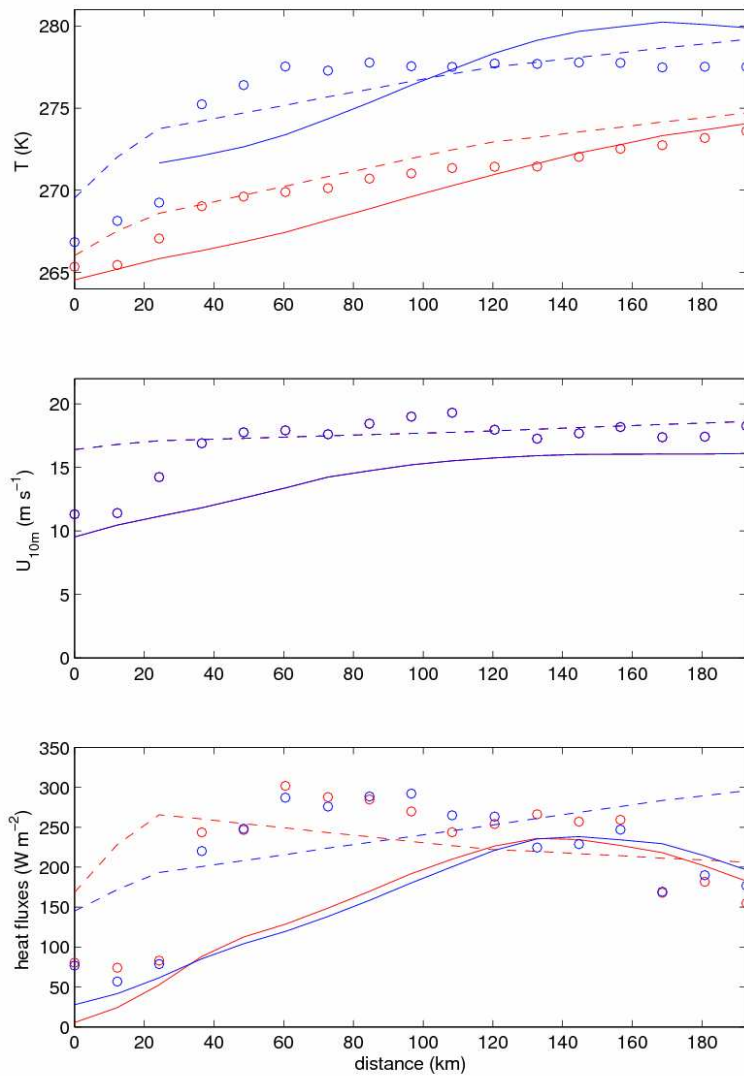
1003

Figure 2. Frequency of winds exceeding 25 m/s for the QuikSCAT observations from July 1999 through June 2009, based on Remote Sensing Systems' Ku2001 algorithm. Statistics are computed by averaging vector winds from the original satellite swath measurements into 0.25° by 0.25° bins. Northern Hemisphere extreme winds are associated with topography (e.g. around Greenland, see Renfrew et al. 2008) and western boundary currents and occur in boreal winter; Southern Hemisphere events are more wide spread and occur year around. Locations with less than approximately 51% of possible observations are plotted as white, thereby excluding some regions with too much seasonal ice.

Flux Accuracies and High Latitude Applications



1004
 1005 **Figure 3.** Spatial and temporal scales for high-latitude processes and the recommended accuracy of
 1006 related surface fluxes. These accuracies are estimates from a wide range of scientists working on
 1007 related processes. The accuracy requirements are difficult to determine or validate, as the modeling and
 1008 observational errors, as well as the validity of assumptions, in current estimates are not sufficiently well
 1009 understood to quantify requirements.



1010

1011 **Figure 4.** Boundary-layer observations of a cold-air outbreak off the east coast of Greenland during an
 1012 instrumented aircraft flight on 5 March 2007, as a function of distance from the coast. Panels show
 1013 (top) 2-m temperature (red) and sea-surface temperature (blue); (middle) 10-meter wind speed; and
 1014 (bottom) surface sensible (red) and latent (blue) heat fluxes calculated using the eddy covariance
 1015 method (taken from Petersen and Renfrew 2009) as a function of distance. The observations are
 1016 averaged into 12-km runs (circles). Interpolated estimates from ECMWF operational analyses (solid
 1017 line) and the much coarser resolution NCEP global reanalyses (dashed line) are also plotted. The plots
 1018 show a rapid warming from over the sea ice zone (0-30 km) off shore and a jump in wind speed and
 1019 observed heat fluxes across the ice edge.

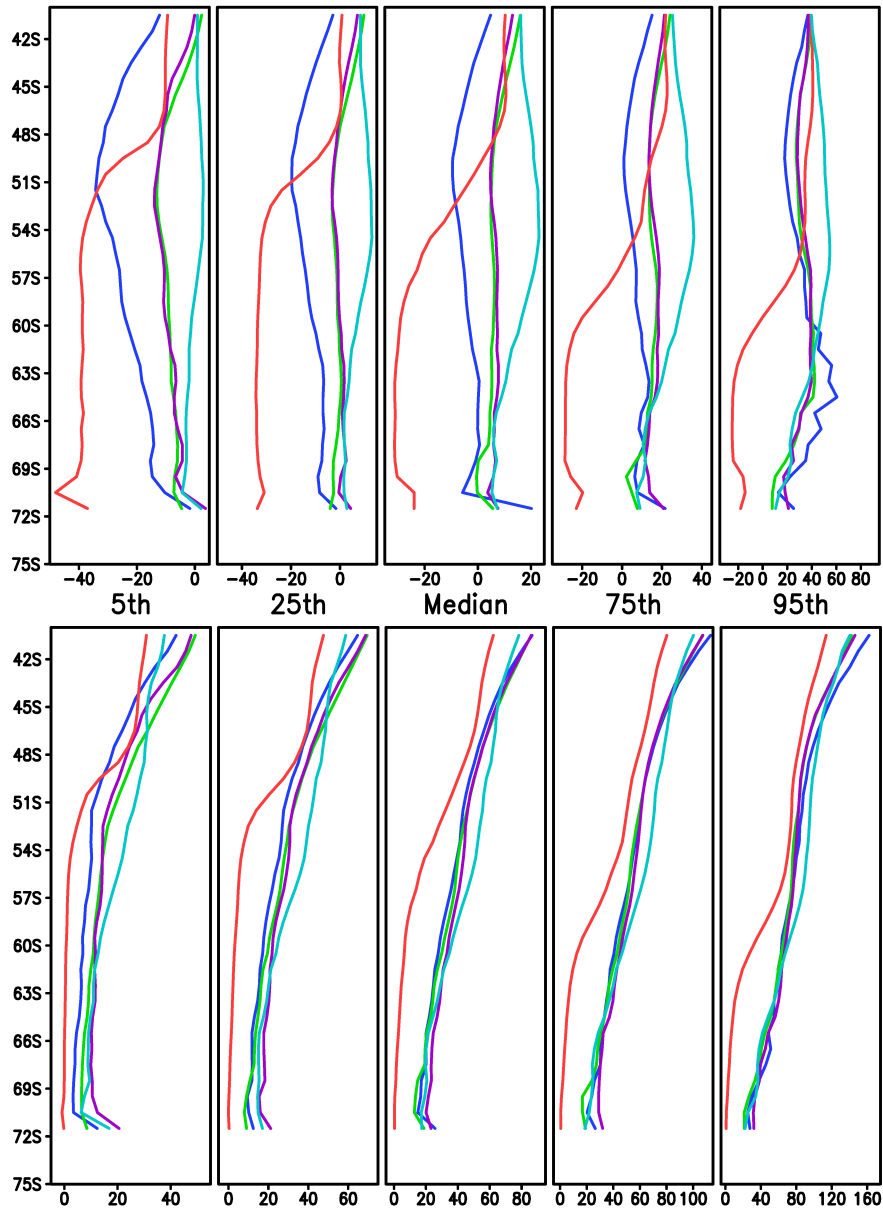


Figure 5. Comparison of oceanic sensible (top) and latent (bottom) heat fluxes from readily available products: NCEP2 (blue), JMA (green), ERA40 (purple), IFREMER (red), and HOAPS (cyan). Each box shows zonally averaged (0 through 360 degrees) monthly fluxes for the 5th, 25th, 50th, 75th, or 95th percentiles. The period for comparison (for which all products are available) is 03/1992 through 12/2000. Clearly there are very large differences in the distribution of fluxes. Note that the range of fluxes (x -axis) is not constant, with the range for the 95th percentile being about 4 times the range for the 5th percentile. Furthermore, there is a great deal of regional surface flux variability in all high latitude seas: product differences are greater on smaller spatial and temporal scales. Details about the data, parameterizations and assumptions used to develop these products are given in Smith et al. (2010).

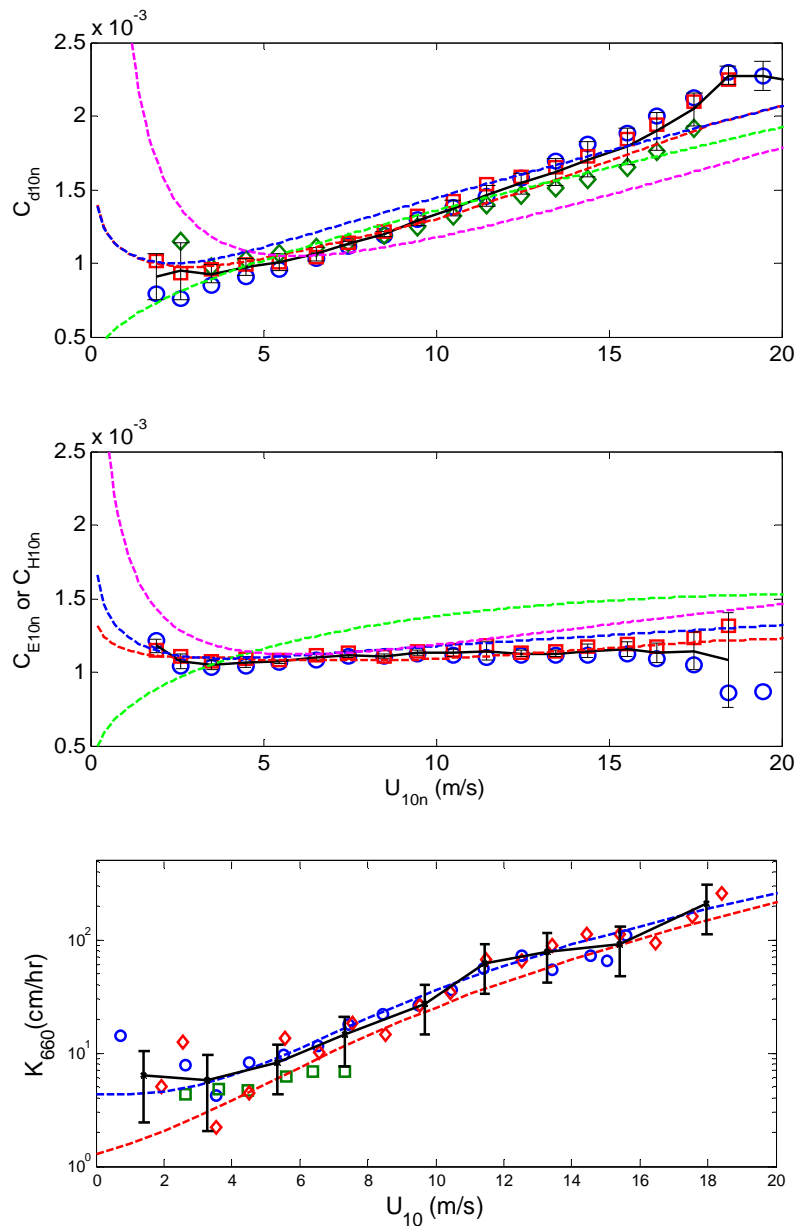


Figure 6. The 10-m neutral turbulent transfer coefficients (C_{d10n} , C_{E10n} , C_{H10n}) and the CO_2 transfer velocity ($K_{660} = C_G |(U_{10} - U_s)|$) as a function of 10-m neutral wind speed from direct surface-based observations: drag coefficient (top), heat transfer coefficients (middle) and CO_2 transfer coefficient (bottom). A percentage error in the transfer coefficient results in a similar percentage error in the flux: differences in parameterizations are greatest at low and high wind speeds. The black line is the mean of

the data sets; the error bars are statistical estimates of the uncertainty in the mean. The parameterizations shown in the top two panels are COARE algorithm (red), NCEP reanalysis (green), ECMWF (blue), Large and Yeager (magenta). Symbols on the upper two panels are: circle – U. Connecticut (FLIP, Martha’s Vineyard Observatory, and moored buoys), diamond – U. Miami (ASIS spar buoy), and square – NOAA/ESRL (ships). The gas transfer coefficient parameterizations shown in the bottom panel are: McGillis et al. 2001 (blue dashed line), NOAA/COARE CO_2 (red dashed line). CO_2 panel symbols are: circle - GASEX98, square - GASEX01, diamond – GASEX08 (data courtesy J. Edson, W. McGillis).

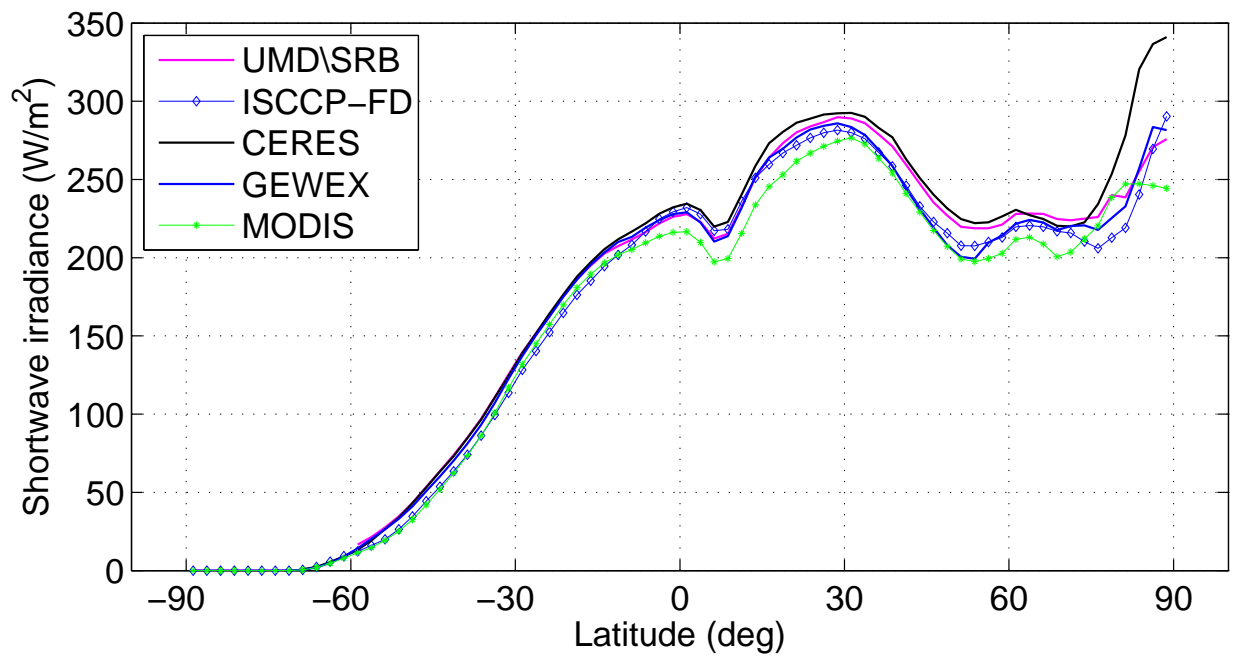


Figure 7. Comparison of the zonal mean downwelling shortwave flux products averaged for two July months (2003 and 2004) from four products: CERES (Wielicki et al., 1996); ISCCP-FD (Zhang et al., 2004); UMD/V3.3.3: and MODIS (Wang and Pinker, 2009). Note the relatively large disagreement in the Northern Hemisphere and particularly the Arctic latitudes.